An Investigation into Numerical Modeling of Gas-Solids Flow in Fluidized Dense Phase Pneumatic Conveying

A Dissertation Submitted
in partial fulfillment of the requirements
for the degree of

Master of Engineering
in
Thermal Engineering

by

Shruti Vikram
Registration No.: 801583024

Under the supervision of

Dr. S.S.Mallick
Associate Professor

Dr. Anu Mittal
Assistant Professor

MECHANICAL ENGINEERING DEPARTMENT

THAPAR UNIVERSITY, PATIALA

July, 2017

Certificate

I hereby declare that the thesis entitled, **"An Investigation into Numerical Modeling of Gas-Solids Flow in Fluidized Dense Phase Pneumatic Conveying"** is an authentic record of my work carried out as per requirements for the award of degree of **Master of Engineering** in **Thermal Engineering** at **Thapar University, Patiala** under the supervision of **Dr. S. S. Mallick** (Associate Professor) and **Dr. Anu Mittal** (Assistant Professor), Mechanical Engineering Department, Thapar University, Patiala during July 2015 to July 2017. No part of the matter embodied in this report has been submitted to any other university or institute for the award of any other degree.

Date: 02/08/2017

Place: Patiala

Shruti Vikram.

Shruti Vikram

801583024

This is to certify that above statement made by the candidate is correct and true to the best of my knowledge.

Dr. S.S. Mallick
(Associate Professor)

Dr. Anu Mittal
(Asst. Professor.)

Department of Mechanical Engineering
Thapar University, Patiala – 147004

Dedication

In the loving memory of

My grandparents late Virendra Singh Arya and late Sushila Devi. I also dedicate this to my Uncle late Khushal Singh, who is an everlasting inspiration in my life.

Acknowledgements

In the phase of life when one has achieved a new milestone, the first feeling that strikes both heart and mind at a lightning fast speed is that may be this tiresome journey had not been possible without the sincere efforts, care, prayers, love and best wishes that others had showered on you at the time you needed them the most and were instrumental in the entire venture. It must be a privilege to make them to be a part of this acknowledgement.

In the first place I would like to pay my sincere gratitude to my supervisor Dr. S.S. Mallick for his supervision, bountiful advice and guidance. His perceptive and expounding qualities helped me to keep myself updated in all the domains. He always motivated and inspired me to achieve new laurels each day and removed most of inhibitions and allowed me to know my shortcomings.

I owe my sincere thanks to my co-supervisor Dr. Anu Mittal for providing me the generous support for the successful completion of my research tenure.

I offer my heartfelt gratitude to Prof. A.K. Lal Sir for his valuable advice and guidance. I would also like to thank all the teachers for their generous support and the guidance at the time when I needed it the most.

I am highly grateful to my sister Krati Vikram and my M.E friends Amrit, Anmol, Bhoopendra Pandey and Rishabh for their generous support.

My parents deserve a special space in this acknowledgement.

I am highly grateful to God who blessed me with such wonderful people in my life, for guiding me well and giving me immense courage and power to accomplish this task.

Abstract

Dense phase pneumatic conveying systems have been associated in numerous mechanical industries for conveying bulk solids through an enclosed conveying line. Dense phase conveying offers potential advantages such as lower energy utilization, decreased particle degradation and pipeline wear as compared to conventional dilute phase conveying.

Fine powders belonging to Geldart group A such as fly-ash, cement, flour etc. are the potential candidates for dense phase pneumatic conveying because they have low de-aeration characteristics. The flow is a highly concentrated dense flow at the bottom of the pipe and dispersed flow at the top of the cross-section.

In the present study, a two layer model is being developed inside a horizontal pipe ignoring the variation of cross-section of the two layers along the length of the pipe. Conservation equations (based on mass and momentum) are solved for both the gas and solid phases by using appropriate coupling parameters. Equations have been solved numerically using Runge –Kutta method and the evolution equations are solved for the flow variables. The flow parameters are calculated along the midpoint sections of the pipeline by ode 45 solver.

Keywords: Dense phase pneumatic conveying, dispersed phase, two layer model MATLAB, Ordinary differential equations, ode 45

Table of Contents

List of Figures

List of Table

Nomenclature

h	Layer height [m]
S_1 , S_2	'wetted' perimeter of the dense and dilute layer [m]
S_i	Length of the interface between the dense and dilute layers. [m]
D	Pipe diameter [m]
D_p	Mean particle diameter [micron]
P	Gas phase pressure [N/m^2]
C_d	Drag coefficients for particles in dense and dilute layer.
F_{dk}	Body forces between the phases in layer k
F	Friction factor
ε_{gk}	Volume fraction of gas in layer k
ε_{sk}	Volume fraction of solids in layer k
S_{mg}	gas-phase mass transfer between the layers
S_{ms}	Solid-phase mass transfer between the layers
R	Universal gas constant
X	Length in flow direction along pipe [m]
Re	Reynolds number of gas
Re_p	Reynolds number of a particle
$U_{\alpha k}$	Velocity of phase α in layer k [m/s]
$\tau_{\alpha k}$	Shear stress between the phase α and the pipe wall in layer k [N/m^2]
$\tau_{\alpha si}$	Shear stress between the phase α in layer 2 and the solids phase in layer 1 [N/m^2]
$T_{\alpha k}$	Temperature of the phase α in layer k [kelvin]

A_1	Portion of cross-sectional area of the pipe occupied by the non-suspension layer in dense-phase regime [m^2]
A_2	Portion of cross-sectional area of the pipe occupied by the suspension layer in dense-phase regime [m^2]
U_{mf}	Minimum fluidization velocity [m/s]
w_{fo}	Single particle settling velocity in undisturbed fluid [m/s]
μ_{air}	Dynamic viscosity of air [N-s/m^2]
ρ_s	Density of the solids particles [kg/m^3]
ρ_{gk}	Density of the gas particles in layer k [kg/m^3]
ρ_{bl}	Loose poured bulk density [kg/m^3]
Fr_m	Mean Froude number related to the section of the pipe.
Fr_{min}	Minimum Froude number at the inlet of the pipe
Fr_p, Fr_s	Particle Froude number based on single particle terminal velocity and particle diameter.
t/h	tonnes/hour

SUBSCRIPTS

1	Dense layer
2	Dilute layer
g	Gas phase
s	Solids phase
b	Bulk phase

Chapter 1

Introduction

1.1 Introduction

Pneumatic conveying is a mode of transporting bulk solids (granular materials, dry bulk materials and powders such as fly ash, cement, flour etc.) with the help of conveying gas or air in an enclosed conveying conduit. The pneumatic conveying system may be positive pressure system or negative pressure system. Pressure differential and the air flow from prime mover are the motive forces for conducting pneumatic conveying. Pneumatic conveying process have numerous benefits over mechanical conveying as: A pneumatic conveying system is constituted with bends to fit around the prevailing equipment or machinery whereas a mechanical conveyor has typical straight path with no bends or fittings which makes it more cumbersome to transport material easily in comparison to pneumatic conveying. Due to bends in pneumatic conveying system, it occupies less space the mechanical conveyor, hence more compact. Very few parts of pneumatic conveying system are moving in comparison to mechanical conveyor; hence comparatively less maintenance is required and also the pneumatic conveying system is closed and compact, so it does not allow any foreign material (dust and debris) to mix with the conveying materials whereas the mechanical conveyor is open to the atmosphere allowing the foreign material to mix with the conveying matter and causing adulteration.

However, there are some drawbacks in pneumatic conveying systems such as larger size of dust collector is required in pneumatic conveying system than mechanical conveyor because separation of material from conveying air in pneumatic conveyor takes place at the end of the system and requirement of more horse power than mechanical conveyor, resulting from the pneumatic system's requirement to alter air pressure to produce conveying power, etc.

A typical positive pressure pneumatic conveying system comprise of the following components.

- The Prime Mover. Mass flow rate and pressure of air, which may be negative or positive are important to convey materials effectively. It can be accomplished by a wide variety of compressors, fans and blowers depending upon the pressure difference required.

- Feeding, Mixing and Acceleration system.

  This zone is considered as the most crucial zone in pneumatic system design. In this zone, material is fed into the pipeline and mixed with the flowing air stream; solids are accelerated from rest to the solid's conveying velocity due to large momentum change and the mixing accompanied with this momentum change is the requirement to provide an acceleration zone. If the physical space allows, the zone normally comprises of a horizontal piece of pipe of a definite length designed such that the solids are accelerated to some 'steady' flow state process occurs. For the efficient working of the system, feeder is chosen which satisfies all the requirements of the solids as well as the system.

  The different types of feeding devices are as follows.

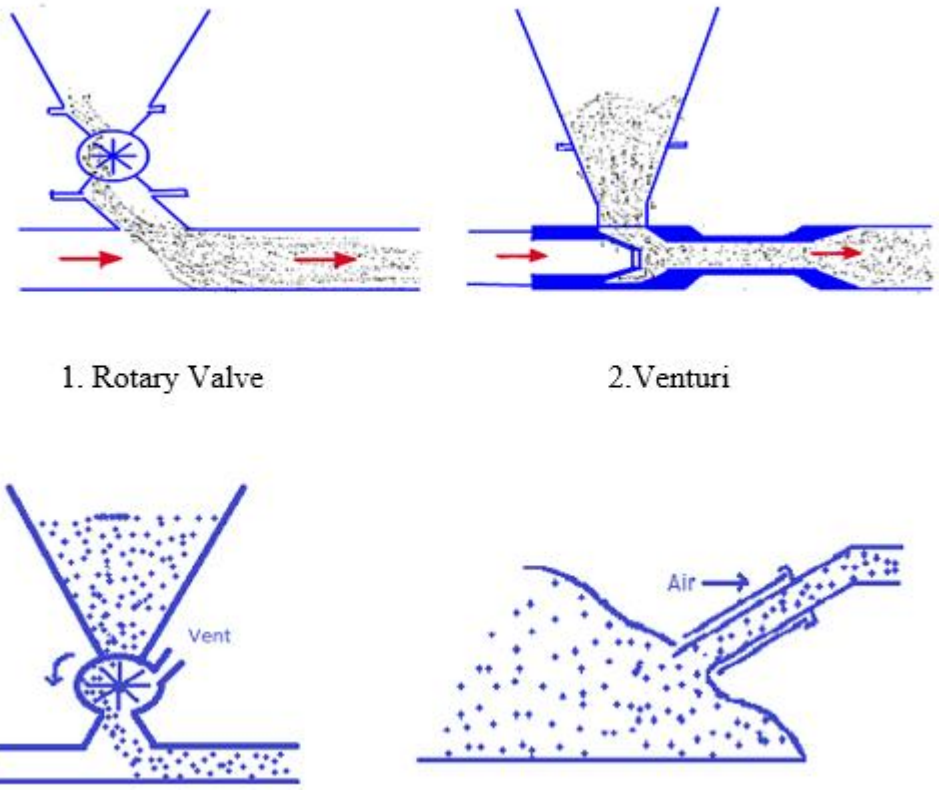

1. Rotary Valve

2.Venturi

3. Screw feeder

4. Vacuum Nozzle

Figure 1.1: Components in pneumatic conveying system

Blow tanks are frequently employed in pneumatic conveying systems since they have capability of using high pressure air. A high pressure air supply is essential if it is required to carry over long distances in dilute phase, or to transport at high mass flow rates over short distances through small diameter pipelines. In maximum blow tank systems, the air feed to the blow tank is divided into two streams. One air stream pressurizes the blow tank and may also fluidize or aerate the material in the blow tank. This air stream assists in releasing the material from the blow tank. The second air stream is supplied directly into the discharge line just downstream of the blow tank. This is commonly denoted as supplementary air and it offers the necessary control over the material flow in the carrying line.

In a top discharge type blow tank, a discharge valve is provided at the top so that it can be separated from the conveying line. It also has a vent line and valve so that it can be de-pressurized without depending on conveying line. Discharge is set through an off-take pipe which is placed above the fluidizing membrane. The material is discharged upright and the discharge pipe departures the blow tank through the top of the vessel, and therefore the term 'top discharge' in this case.

In a bottom discharge blow tank, there is no membrane. Material has a continuous passage without any interruption to be gravity fed into the pipeline and so the contents can be completely discharged.

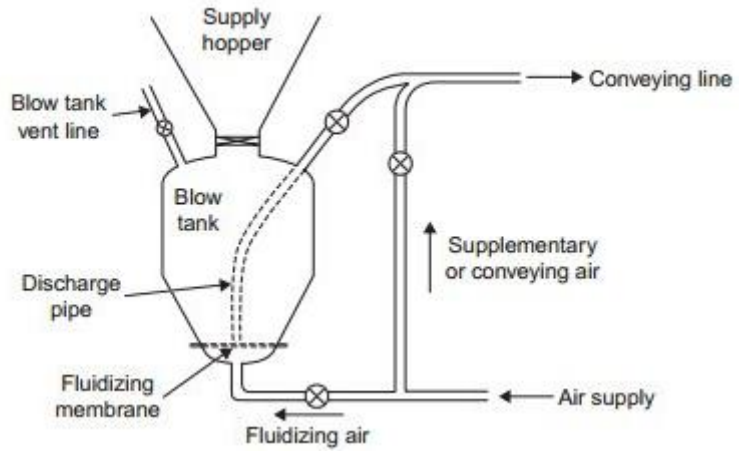

Figure 1.2: Top discharge blow tank with fluidizing membrane

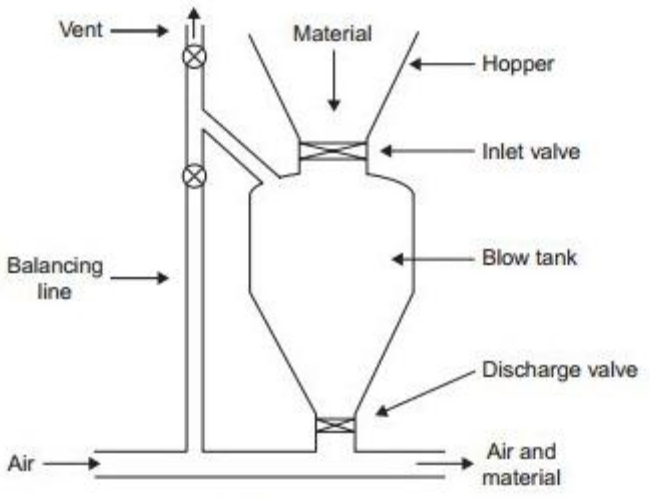

Figure 1.3: Bottom discharge blow tank

Blow tanks can feed up to 500k Pa (and even higher up to 5000kPa in some cases like coal gasification etc.). The blow tank has stationary parts and so both wear of the feeder and degradation of the material are considerably reduced

- Conveying line

  Once solid is accelerated, it enters the conveying zone which consists of bends, pipes, joints etc. The choice of conveying line material depends on the pressure drop and particle properties. The pipe material should be chosen in a way that the friction losses and particle degradation in it are minimum.

- Separating devices

  Here conveying gas is separated from the particles with the help of cyclones or bag filters. The selection of gas-solids separators depends on numerous factors, the primary factor being the size of the particles which have to be parted from gas streams.

  Cyclones are gravity based so these are used for heavyweight particles and bag filters are employed for fine powders. If the solid material has a broad particle size distribution, then both cyclones and bag filters can be utilized and bag filters are placed next to the cyclones.

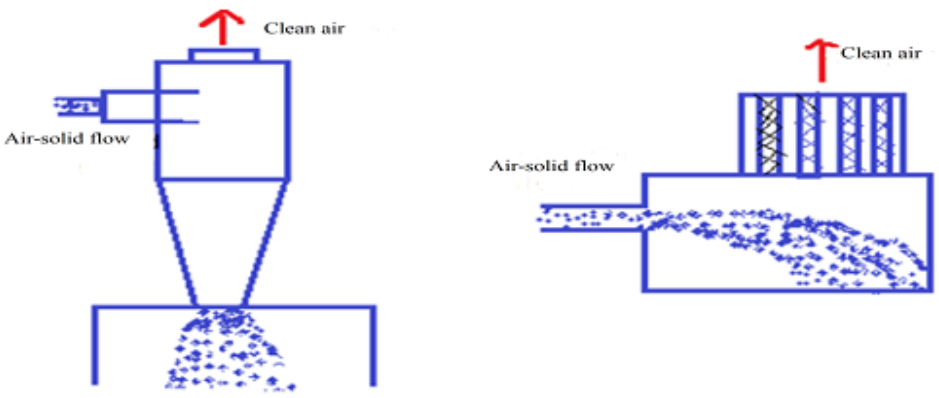

Figure 1.4: Separating Device

On the basis of operating principles, pneumatic conveying is categorized into two types: Dense and Dilute. Either can run under pressure or vacuum.

Dilute Phase: In dilute phase pneumatic conveying, the particles are aerated, i.e. particles are fully suspended in air. Due to that, a relatively high conveying velocity and relatively low pressure is required along the length of pipeline. The velocity of air is maintained according to the type of solid particles to be to be conveyed.

The most common method of conveying granules and powders is 'dilute phase pressure conveying'. It is mostly applicable for the particles which have light bulk density (typically of the order of 62 lb. $/ft^3$). The particles should be non-abrasive and non-fragile. Common examples are, flour, zinc oxide etc.

In 'dilute phase vacuum conveying' the conveying materials are compressed or packed under pressure. Examples include, wood shavings, fibrous materials and certain toxic materials that should not leak to the surrounding air. This system is normally used to transport materials over definite short distances at small capacities. Dilute phase vacuum conveying is best for transporting material from several sources to a single final destination.

Dense Phase: In dense phase pneumatic conveying, the particles are not fully suspended in air and they tend to flow in the form of dunes. Dune flow is basically moving bed flow, in which solid particles are transported in the form of dunes along the pipeline at the bottom.

‘Dense phase pressure conveying’ is appropriate for conveying brittle and delicate materials with average particle size ¾ inch and smaller over large distances (more than 250 feet).Commonly handled materials are silica, fly ash, resins etc. Low velocity conveying of materials is conducted to prevent the materials from degradation and prevention of abrasion in pipeline, bend.

‘Dense-phase vacuum conveying’ is best suited for the transportation of fragile materials up to short distances. This system transports granules or powders at low rate (25 t/h or less) in applications like truck unloading etc.

The dense phase flow can be further classified into:

1. Plug/slug flow (particle diameter > 500 µm)
2. Fluidized dense phase flow

Heavy pressure fluctuations and pipeline vibrations occur due to the conversion of granular particles from dilute to dense phase or vice versa in the plug/ slug flow(particle diameter > 500 µm) (Williams 2008).

On the other hand, in fluidized dense phase flow (particle diameter < 100 µm), the flow transition of fine particles from dilute to dense phase is very smooth which is attributable the high air retention capability (Williams 2008).

In spite of having a number of benefits, designing of fluidized dense phase pneumatic conveying system poses certain challenges because the highly turbulent fluidized bed involves complex interactions such as particle to particle, particle to wall and particle to air. So, researchers have heavily relied upon the empirical models for determining the pressure drop through the pipeline. As of now, a very little work has been attempted for developing the fundamental understanding of flow mode mechanisms especially for fluidized dense phase pneumatic conveying. In view of this, an attempt has been made to develop and solve the fundamental governing equations for solid-gas flow during fluidized dense phase conveying of fine powders.

1.2 Objectives

In view of the limitations, further studies are to be conducted as follows:

1. Formulation and solving of fundamental equations for gas and solid phases individually in dense and dilute modes of flow (Based upon mass and momentum balance) using appropriate coupling terms such as drag coefficient, interlayer momentum transfer etc.

2. Deciding the appropriate boundary conditions depending upon geometry and operating variables.

3. Constructing evolution equations of the coupled nonlinear equations for the parameters

4. Solution of the evolution equations in MATLAB and to study the variation of flow parametersU_{s1},U_{g1}, ε_{s1}, ε_{g1},U_{s2},U_{g2}, ε_{s2}, ε_{g2} along the length of pipeline

Chapter 2

Literature Review

2.1 Introduction

Fluidisation is the phenomenon of mixing of the bulk particles with gas such that they behave like fluid. The minimum velocity required to suspend the particles in air and flow like fluid is called minimum fluidisation velocity U_{mf} .Fluidized dense phase is more complex in nature; it is visualized in two layers, dispersed phase layer on upper section and dense phase layer on bottom section of the pipe. Both dispersed phase and dense phase show discrete flow patterns. Based on gas-flow velocity, transport rate, pipe roughness and diameter, the flow pattern in dense phase can vary from stable dune flow to low velocity slug flow [Wypch, 2006].In dilute phase flow, large volumes of air at high velocity is supplied sufficient enough to carry the particles in full suspension [Klinzing et al., 2009].Reduction in flow velocity leads to non-suspension of particles and thus forming dense mode of flow.

2.2 Geldart's classification Diagram

Geldart [1973] developed a diagram for the classification of bulk materials (Figure 2.1) that calculates the ability of pneumatic conveying. The diagram shows the categorisation of bulk materials into any of the groups Geldart A, B, C or D on the base of mean particle diameter and the difference between particle density and gas density. On the basis of the fluidisation characteristics of particles, the material can be characterised in any of this group classification.

Group A: These particles have good air retaining capacity and hence favourable for fluidised dense flow. The collapse of the fluidised dense flow is very gradual when the carrier air flow supply is stopped. In these materials, bubbles may appear later on after fluidisation. Examples include cement, fly ash etc.

Group B: These materials have poor permeability as compared to the materials of Geldart A group. The materials are granular in nature therefore they have low air retention capability. As the gas supply is turned off, the fluidised bed collapses quickly. Bubbles can be observed in the fluidised bed at or slightly above minimum fluidisation velocity. Examples, Sugar granules and limestone dust etc.

Group C: The materials belonging to this group are very fine and extremely cohesive in nature. Fluidisation of Geldart C group materials is difficult but once the particles are aerated, they are

most suitable for fluidised dense phase flow. Problem in fluidisation is in the form of lifting plug of bulk materials or vertical and inclined cracks. Examples include fly ash, talcum powder etc.

Group D: These materials are highly granular in nature and are tough to fluidize because of high permeability. Minimum fluidisation velocity required for these particles are comparatively high than those of Geldart group B particles. Examples include wheat kernels, mustard seeds etc.

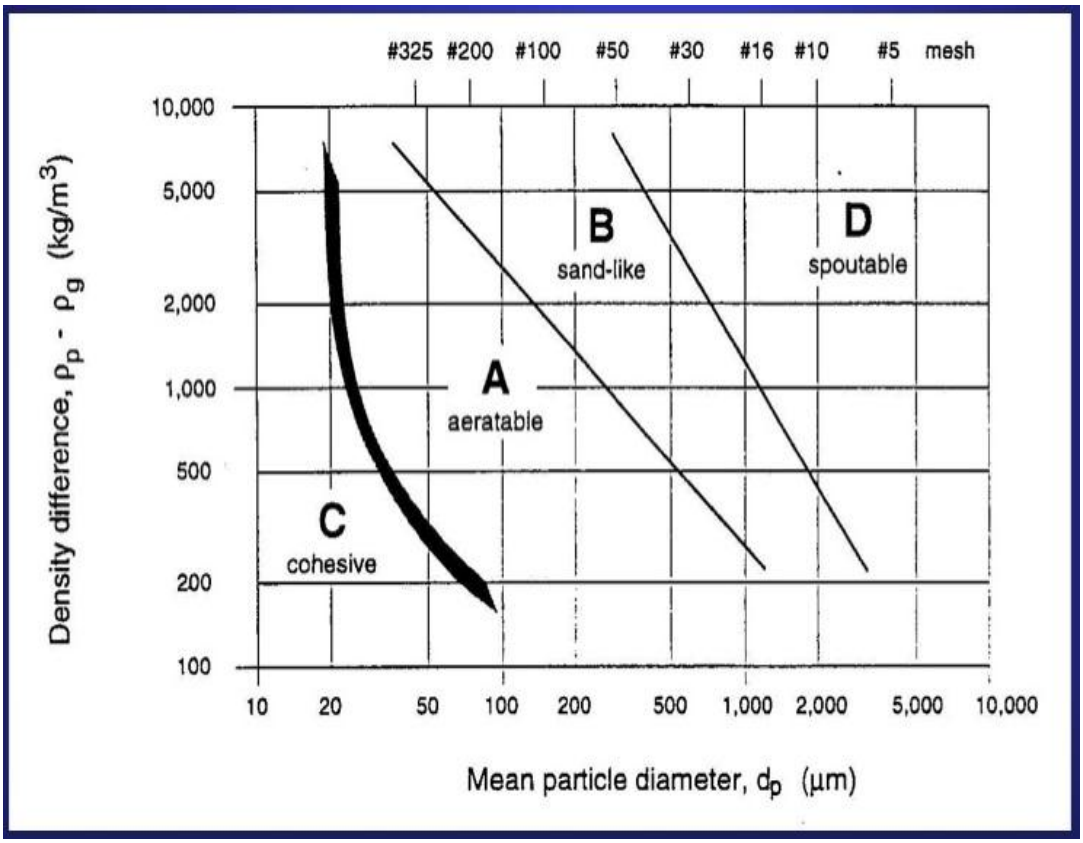

Figure 2.1: Fluidisation Classification Diagram [Geldart, 1973]

2.3 Previous Research Work

Various researchers provide literature on fluidisation phenomenon. The study comprises the behaviour of flow modes of dense phase and dilute phase.

[Xu et al., 2016] built up another model for least fluidization speed for fine powders of different level of cohesiveness in light of Ergun condition and the compel adjust of a particle bed under fluidization bringing into record the inter particle strengths.

Least fluidization speed U_{mf} is the important parameter to depict fluidization of particles. Least fluidization is characterized as the state at which the heaviness of entire bed of particles starts to be totally bolstered by the fluidizing gas, and the weight drop of the gas over the bed winds up plainly steady with expanding gas speed. The fundamental target of the analyst was to build up another relationship to foresee U_{mf} for fine particles by considering the interparticle powers. A relationship between base fluidization voidage $\varepsilon_{mf}$and molecule size was likewise gotten from trial information.

The review proposed that for fine or firm particles, (Geldart C and Geldart C/A powders) where the interparticle strengths are moderately critical, the durable constrain impact of molecule size on ε_{mf} , and thus U_{mf} needs to be considered.

[Behera et al., 2013] did simulation by continuum approach in order to predict different flow parameters of dilute phase conveying through pipe. Governing equations (Continuity, momentum and energy equation) were solved with known exit boundary conditions by using MATLAB coding. Granular particle is assumed as granular gas, characterized by granular temperature and this parameter was included in energy equation. The results showed the variation of absolute pressure and granular temperature along the length of pipe for discrete values of tangential and normal restitution coefficients.

[Behera et al., 2012] suggested a different approach to modeling fluidized dense phase conveying. The author used governing equations (continuity and momentum equations) to predict inlet flow parameters (pressure drop and mass flow rate of air) of pipeline. These equations are solved for single gas phase particles (depending upon particle size distributions). Initially author guessed the area factor (aa:"varies from 11 to 50") and friction coefficient (γ:" varies from 0.05 to 0.09") of solid phases. Experimental data of four different materials (two qualities of fly ash and two qualities of alumina) was used to compare predicted values and hence optimized area factor and friction coefficient for each material. The author used the minimum Froude number value for inlet boundary conditions given by [Mallick and Wypych, 2009], for reliable conveying. The results showed that friction coefficient varies linearly with the ratio of particle density to the mean particle size. [Mills et al.,1982] and [Arnold et al.,1986] proposed scaling specific correlations for air and solid mass flow rate that was used to analyse pressure drop of changed length and diameter.

[Sundaresan et al., 2003] developed a frictional kinetic model for dense assemblies of solids in a gas-particle mixture. Kinetic and frictional stresses were taken additive in this model. Particulate stresses in dense phase flow were generated by frictional interactions between particlesatpointsofsustainedcontact.Sincefrictionalstressesplayaveryimportantrolein many dense phase gas-solid flows e.g.it was shown in the paper that frictional stresses play a critical role in maintaining stable operation of circulating fluidized bed. The kinetic stresses were based on the kinetic theory of granular materials, which likewise considered the impacts of the interstitial gas. For calculating the frictional stress, the model proposed by Schaeffer was implemented.

[Wang et al., 1997] directed examinations on the fluidization of fine particles (Geldart Group C) extending with normal sizes 0.01 micrometre to 18 micrometres and densities fluctuating from100 to 8600kg/m^3. Whenever fluidized, the elements fluidized for the most part comprise of particle agglomerates shifting in size from biggest at the base of the bed to the smallest size at the top. Bringing agglomerate density ends up being a powerful measure for enhancing the fluidization nature of fine powders. Consequences of simulations of the two model issues the gravity release of particles from the bin and the ascent of the rise in fluidized bed was introduced. The simulations caught the height free rate of release of particles from the bin, the event of pressure deficiency over the whole, the expansion of molecule gathering close to the exit orifice and the critical impact of frictional stresses of the interstitial air on the release conduct of fine particles. The bubbles rise case demonstrated the huge impact of frictional stresses on the bubble shape. The solids fluidized comprise of molecule agglomerates circulating into the biggest size at the base of the bed to the littlest at the top when fluidized.
The conclusions from Wang theory were:

1. Diverting, disturbing, plugging and coagulation are the essential practices of fluidization particles.
2. Single particles, common agglomerates, and fluidized agglomerates are the three phases of fine particles.
3. Fluidization character of fine agglomerates can be subdivided into four classes slugging and directing; agglomerate fluidization like Geldart group A particles; agglomerate fluidization like Geldart group B or D particles; transitional as agglomerates fluctuate in size with operation.

4. The bigger agglomerates at the base of the bed were include littler of the parent singular particles, while the littler agglomerates additionally up in the bed comprise of the bigger individuals from the parent discrete particles.

[Hong et al., 1993] built up a physical model for gas—strong stratified stream with high solids/gas mass flow rate proportion (supposed solids stacking) in even pneumatic conveying on the basis of understanding the contact mechanism amongst suspension and sliding bed, . It was bring into being that the anticipated pressure drop from the created show agrees inside ±30% with the exploratory information for carrying medium size sand and fine lime in an 8 m long pipe with a distance across of 20 mm under an extensive variety of solids stacking from 30 to 200. Additionally, calculations for phase outline, flow setup and speed of sliding bed appear to be more sensible from the present model than past models.

The empirical correlations for solids friction factor and fluid friction factor developed by researchers also have been discussed in this chapter. Numerous researchers have worked on the formulation of empirical models. However, very few researchers have used numerical simulation method to study the effect of friction factors on flow parameters.

[Patwardhan, V.S. and Tien, C., 1985] studied the behaviour of fluidization and sedimentation of the powders of varying sizes and densities. A new theory of "Apparent porosity of suspensions" was evolved and equations could be developed that were able of calculating the settling velocities of discrete particle in a suspension comprising mixture of particles. The equations were validated against experiments held against fluidization and sedimentation.

According to [Richardson and Shabi, 1960], the settling velocity for the sedimentation of suspension of particles of dissimilar sizes and alike density is given by formula

$$U_i = F_\varepsilon$$

Where, U_i is the fraction of the relative velocity of the particle (with respect to the liquid medium) to the terminal velocity of a single particle of the similar kind. F_ε Is a function of the permeability of the suspension (or particles concentration).

- Solids Friction Factors ($\boldsymbol{\lambda_s}$)

Solid friction factor is an important parameter in predicting the pressure drop in fluidized dense phase pneumatic conveying. The correlations for dilute phase of solids friction factors (λ_s) have been well defined in the literature. Many researchers' empirical correlations are illustrated

below in table. Out of these correlations, only one, Setia et al. (2016) proposed a two layer model of solid friction factor for fluidized dense phase.

As (solid friction factor) is the function of dimensionless terms such as Froude number, mass loading ratio, velocity ratio, density ratio, volumetric loading ratio, diametrical ratio etc.

Table 2.1: Different solid friction models

Author	**Models**
Stegmair (1978)	$\lambda_s = 2.1\ m^{*-0.3} Fr_m^{-2}\ Fr_s^{0.5}\ (D/d_s)^{0.1}$
Rizk (1982)	$\lambda_s = \lambda_s^* C/V + 2\beta/\{(Fr^2\}C/V)$
Pan and Wypych (1998)	$\lambda_s = 3.2343\ (m^*)^{-0.47}\ (Fr_m)^{-1.56}\ (\rho_m)^{-0.43}$
Jones and Willams (2003)	$\lambda_s = 83/\{(m^*)^{0.9}\ Fr_i^2\}$
Willams and Jones (2004)	$\lambda_s = K(m^*)^a\ (Fr_m)^b$
Setia (2015)	$\lambda_s = K\ (\frac{W_{f0}}{V})^a (VLR)^b$
Setia (2016)	$\lambda_s = \tau_1 \left[(VLR)^a \left(\frac{W_{f0}}{V} \right)^b \right] \times \tau_2 \left[\lambda_s^* \frac{C}{V} + 2\beta_0/\{(C/V)Fr^2\} \right]$

- Friction Factor for Fluid

  In 1944, Lewis Ferry Moody plotted the Darcy–Weisbach friction factor against Reynolds number Re for various values of relative roughness ε / *D*

  $\lambda_f = \frac{64}{Re}$ For Re≤ 2100 (laminar flow) where Re =$\frac{v\rho D}{\mu}$

  $\lambda_f = \frac{1.325}{\left[\left(\ln\left[\frac{€}{3.7D} + \frac{5.74}{Re^{0.9}}\right]\right)\right]^2}$ For $5000 \leq Re \leq 10^8$(turbulent flow) and $10^{-6} \leq \frac{e}{D} \leq 10^{-2}$

  Where D = Diameter of a circular duct

  Re = Reynolds Number

  If duct is non-circular, then D is computed as the hydraulic diameter of a rectangular duct, where D = 4A / P.

[**Shampine et al., 1997]** described the mathematical modeling for the suit of programs for solving initial values problems in MATLAB basically for ordinary differential equations. In this paper, implicit formulas for stiff systems, the numerical differentiation formula and method to change step size, linearly implicit formulae and explicit formulae for non-stiff systems has been explained.

By comparing new Runge-Kutta codes with old MATLAB codes, it was observed that NDF code is as popular as BDF code written in FORTRAN.

From the experiments, it was concluded that for solving complex non-linear equations ODE 45 code should be given priority. If the problem is stiff or the problem is unexpectedly difficult for ODE 45, ODE 15s code should be implemented. However, the accuracy of ODE 45 solver is higher than of ODE 15s solver. When solving stiff problems, it is important to keep in mind the options that improve the efficiency of forming Jacobians so as to get maximum accuracte results.

[David Houcque, 2008] described how to use the built in functions available in MATLAB. A detailed explanation for Runge-Kutta method has been presented with the built in MATLAB software ode45.

An ordinary differential equation consists of an independent variable, a dependent variable and the derivatives of the dependent variable.

For solving the initial value problems by numerical method, the modified RK varies the step size, choosing the step size at each step in an orderto achieve the desired accuracy and remove errors. Therefore, the solver ode45 is appropriate for wide arrays of initial value problems in practical applications. In general, ode45 is the excellent function to be relevant as a "first try" for most problems.

Ode45 is based on an explicit Runge-Kutta (4, 5) formula, the Dormand-Prince pair given by Dormand-Prince (1980). That means the numerical solver ode45 combines a fourth order method and a fifth order method, both of which are similar to the classical fourth order Runge-Kutta (RK) method.

The solver can be used with the following syntax:

[x, y] = ode45 (@odefun, tspan, y0)

The concluding points of these studies are listed below:

1. Most of the researchers have developed empirical models for the solid friction factors and fluid friction factor for the dilute flow and less study has been conducted to analyse the friction factors for fluidized dense phase pneumatic conveying of fine powders.
2. Solids friction factor values are different for different conveying materials. Friction coefficient varies linearly with the ratio of particle density to the mean particle size.

3. The cohesive force effect of particles on minimum fluidization voidage result in minimum fluidization velocity prediction. For fine particles where inter-particle forces are significant, the cohesive-force effect should be taken into account in prediction of minimum fluidization velocity.
4. Kinetic and frictional stresses act among the gas solid particles in fluidized dense phase flow. Particulate stresses in dense phase flow are generated by frictional interactions between particles at points of sustained contact. Since frictional stresses play a very important role in many dense phase gas-solid flowse.g.it was shown in the paper that frictional stresses play a critical role in maintaining stable operation of circulating fluidized bed.
5. Ode45 is a useful ODE solver and is the first solver to be tried for most of the problems. For solving the initial value problems by numerical method, the modified RK varies the step size, choosing the step size at each step in an order to achieve the desired accuracy and remove errors.

   Most of the available literature includes the use of empirical correlations for calculating the various flow parameters in dilute phase flow. However, very few literature is available for the calculations of flow parameters for fluidised dense phase by using fundamental equations of physics. The present study has been done for calculating the various flow parameters in a fluidised dense phase by using fundamental equations of physics called governing equations.

Chapter 3

Model Development for Fluidised Dense Phase

3.1 Introduction

Fluidised dense phase model was developed by Wilson (1998) for the flow considering density variations in vertical directions, i.e. the flow is stratified. The model developed is a one-dimensional model, in which two layers of flow inside the pipe are described. In every layer, the gas solid particles are considered to be in one single phase. Shear forces at the interface are considered due to which momentum transfer between the layers was observed. Each layer has a distinct flow velocity. Since the transport fluid is incompressible, the depth of every layer remains constant. However, experimentally it is observed that a substantial change in the depth of layer takes place as the transport fluid expands.

The granular products (particle diameter>500 µm) and with small size distributions, transport as distinct plugs along the length of pipe with the plug diameter being roughly equal to that of the bore of pipe (Jones 1988).Whereas in the case of fine particles (particle diameter < 100 µm), particles convey in a wave like motion at the bottom of pipeline constituting the fluidized dense phase flow as shown in the figure 3.1. It makes suspension and non-suspension layer, the majority of particles transport in the non-suspension layer.

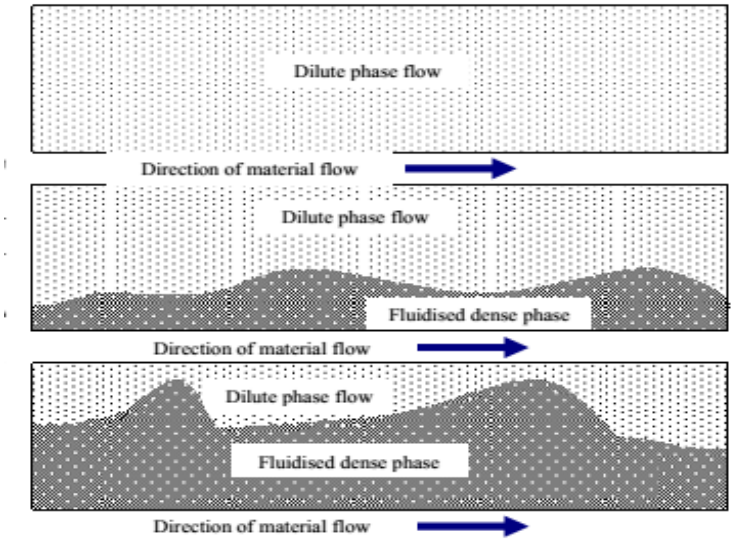

Figure 3.1: Dilute to dense phase transition (Williams, 2008)

Another group of model was developed by [Bohnet, 1965] to describe the role of force balance in order to calculate the pressure drop in a pipe consisting of stratified gas solids flow. The

approach involves modeling the friction forces in dilute layer by the additional wall friction factor whereas Coulomb friction was considered in the dense phase due to the weight of the layer.
[Muschelknaultz and Wojahn, 1974] improved the [Bohnet, 1965] model by considering the effect of shear forces which occur due to the contact between the dense and dispersed layers.
[Wirth and Molerus,1981] developed a steady state model for two layers and calculated pressure drop by considering the force balance on every layer. In this developed model, few assumptions were made which were: all the solids are conveyed in the bottom layer; the slip velocity between the phases in lower layer is insignificant; and the gas phase is incompressible. As a result, the velocity of gas in the top layer is assumed to be constant. On the basis of this model, the stability limits of moving bed type flow were established.
This model was further refined by [Hong and Tomita, 1993] and [Hong and Zhu, 1997] by considering the nature of impacts of particles on the dense layer and their successive rebound or settling.
In the present study, a fluidised dense phase model has been developed (particle diameter =30 µm) for modeling moving bed gas solids flow inside the horizontal pipeline. The geometric parameters used in the model are illustrated in figure 3.2.

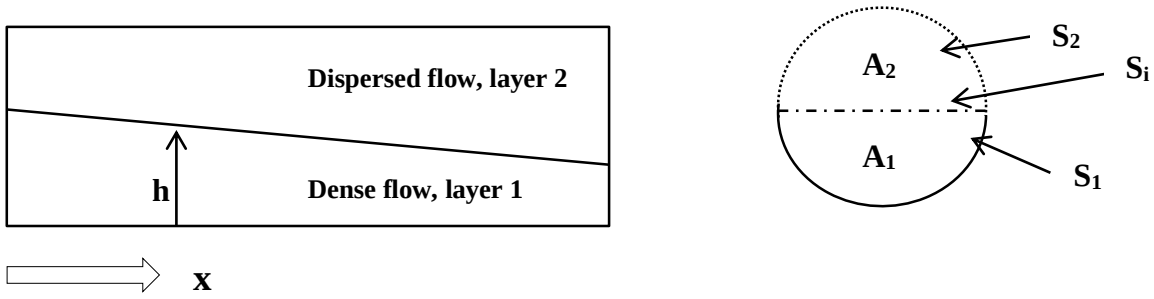

Figure 3.2: The geometric specifications

The height of the layer, h, changes because of the mass transference between the dense and dispersed layers which can take place in both the directions.
For the isothermal flow of solids-gas mixture, the density of the gas phase drops along the length of the pipeline due to gradually decreasing pressure. Therefore, the gas velocities in both the layers must rise in order to fulfil the continuity law. As a result, mass is transported from dense layer to dispersed layer and height of bottom layer decreases. This causes change in cross sectional area.
However, the change in height in the pipes of very small diameter is less so the change in the cross-sectional area along the length cannot be of much significance.

In the present work, change in the height of the lower layer is considered. To select the height of the lower layer, two values are used: 0.8D and 0.2D and the pipeline is divided into 7 segments

Calculation of variation of height with respect to pipe length segment:

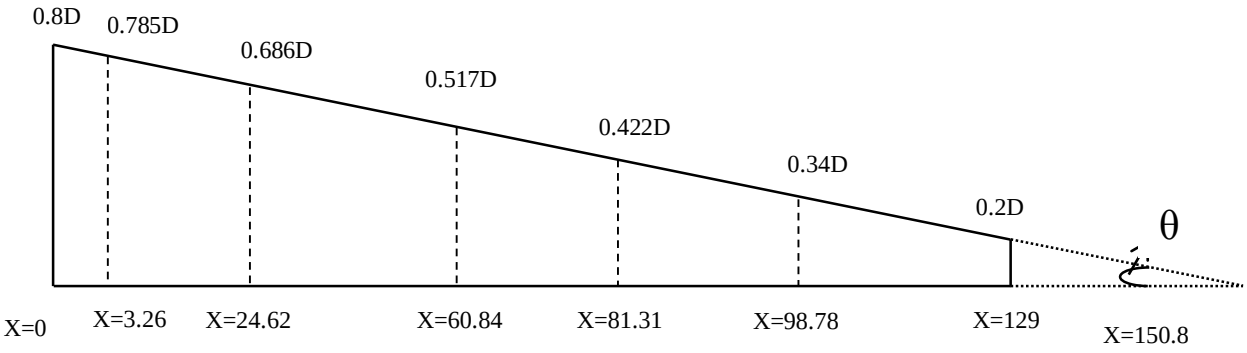

Figure 3.3: Variation of height of bottom layer with respect to flow direction

Calculation of θ:

Tan θ= dh/ dx

From figure,

L=129m

Tan θ = (0.8D-0.2D)/ 129

Tan θ = 0.6D/129

D=69 mm= $69*10^{-3}$ m

Therefore,

Tan θ = $(0.6 *69*10^{-3})/129$;

Tan θ= 0.000321

dh/ dx =0.000321

Thus, by geometry the slope of the lower layer is calculated which gives the variation of bed height of lower layer with respect to the flow length direction

The main feature of this mode of gas-solids flow is the height of the dense layer (Figure 3.2; layer 1).Thus all geometric parameters that influence mass and momentum transfer between the layers and other boundary conditions are being expressed in terms of height. The perimeters written as the function of the dense layer height are:

$\mathring{S} = \frac{S_i}{D} = 2(h. - h^2)\text{^}0.5$ (3.1)

$\mathring{S}1=\frac{S1}{D}$= cos (1-2h.) (3.2)

Where h. (=H/D) is the height of the non-dimensional dense layer and D is the diameter of the pipe. For each layer in the pipe, the volume fraction is defined as:

$\varepsilon_{s1} + \varepsilon_{a1} = 1$ (3.3)

$\varepsilon_{s2} + \varepsilon_{a2} = 1$ (3.4)

In writing the balance equations, the assumptions made are-

1. Flow is one-dimensional (x- direction).
2. Flow is steady.
3. The flow is isothermal.
4. The gas obeys the ideal gas equation of state.
5. The friction force between the gas phase in the bottom thick layer and solids phase in upper thin layer at the common interface S_i is negligible.
6. The flow variation across the cross section of the pipe is negligibly small.
7. The pipe is straight, no inclination and bends are taken into consideration.
8. There are 100% solids and 0% gas particles along the pipe wall boundary in dense phase.
9. There is 100% gas and 0% solid particles along the pipe wall boundary in dilute phase.

3.2 Basic Governing Equations

- Mass balance equations for the gas and solid phase:

$\frac{d}{dx}(\rho_{g1}\varepsilon_{g1}A_1U_{g1}) = S_{mg}$ (3.5)

$\frac{d}{dx}(\rho_{s1}\varepsilon_{s1}A_1U_{s1}) = S_{ms}$ (3.6)

$\frac{d}{dx}(\rho_{g2}\varepsilon_{g2}A_2U_{g2}) = - S_{mg}$ (3.7)

$\frac{d}{dx}(\rho_{s2}\varepsilon_{s2}A_2U_{s2}) = - S_{ms}$ (3.8)

- Momentum Balance equations for the gas and solid phases-

$\frac{d}{dx}(\rho_{g1}\varepsilon_{g1}A_1U_{g1}^2) = S_{mg}U_{g1} - \varepsilon_{g1}A_1\frac{dP_1}{dx} + F_{d1}$ (3.9)

$\frac{d}{dx}(\rho_s\varepsilon_{s1}A_1U_{s1}^2) = S_{ms}U_{s1} - \tau_{s1}\varepsilon_{s1}S_1 + (\varepsilon_{g2}\tau_{gsi} + \varepsilon_{s2}\tau_{ssi})\varepsilon_{s1}S_i - \varepsilon_{s1}A_1\frac{dP1}{dx} + F_{d1}$ (3.10)

$\frac{d}{dx}(\rho_{g2}\varepsilon_{g2}A_2U_{g2}^2) = -S_{mg}U_{g1} - \tau_{g2}\varepsilon_{g2}S_2 - \varepsilon_{s1}\varepsilon_{g2}\tau_{gsi}S_i - \varepsilon_{g2}A_2\frac{dP_2}{dx} - F_{d2}$ (3.11)

$$\frac{d}{dx}(\rho_s \varepsilon_{s2} A_2 U_{s2}^2) = -S_{ms} U_{s1} - \tau_{s1} \varepsilon_{s1} S_1 \ - \varepsilon_{s2} \tau_{ssi} \varepsilon_{s1} S_i - \varepsilon_{s2} A_2 \frac{dP_2}{dx} - F_{d2} \quad (3.12)$$

3.2.1 Complimentary Equations

For the solution of the above governing equations, some complimentary equations are required for: mass transfer, friction forces, body forces and equations of state.

- Mass transfer:

  Mass exchange happens as a result of particles lifting from or settling on the dense layer; and the pressure difference in a pipeline cross-section. At the point when the particles are lifted from the dense layer, the gas that was containing in the voids between the particles is additionally transported to the upper layer. In the present work, the mass exchange because of pressure difference in a pipe cross-segment is disregarded. The mass exchange terms for both the gas phase and solid phase (S_{mg} and S_{ms} respectively) are ascertained from the mass flow of the phase through the area change happened because of the adjustment in height of the dense layer

  $$S_{mg} = \frac{1}{2} \rho_{g1} \varepsilon_{g1} U_{g1} S_i \frac{dh}{dx} \quad (3.13)$$

  $$S_{ms} = \frac{1}{2} \rho_s \varepsilon_{s1} U_{s1} S_i \frac{dh}{dx} \quad (3.14)$$

- Friction forces: The friction forces per unit length for a phase are figured by the product of friction area per unit length by the shear stress between the phase and the layer boundaries. Following set of formulation is used to calculate the shear stress as a function of relative speeds and friction factors:

  Shear stress between the gas phase in dilute layer 2 and solids phase in dense layer 1:

  $$\tau_{gsi} = f_{gi} \frac{1}{2} \rho_{g2} (U_{g2} - U_{s1})^2 \quad (3.15)$$

  Shear stress between the solids phase in dilute layer 2 and solids phase in dense layer 1:

  $$\tau_{ssi} = f_{si} \frac{1}{2} \rho_s (U_{s2} - U_{s1})^2 \quad (3.16)$$

  Shear stress between the solids phase in dense layer 1 and pipe wall

  $$\tau_{s1} = f_{s1} \frac{1}{2} \rho_s (U_{s1})^2 \quad (3.17)$$

  Shear stress between the gas phase in dense layer 2 and pipe wall:

$$\tau_{g2} = f_{g2} \frac{1}{2} \rho_{g2} \left(U_{g2}\right)^2 \quad (3.18)$$

- **Equation of state:**

  In this study, cross-sectional pressure is assumed to be uniform. As a result gas pressure in the entire phase is uniform. The gas phase is assumed to be an ideal gas in every layer i.e.

  $$P = \rho_{g1} RT = \rho_{g2} RT \quad (3.19)$$

  Thus we can conclude that the gas phases in both the layers have equal density.

- **Fluid-particles interaction:**

  The drag forces per unit length are calculated as the product of drag force on a particle and the number of particles per unit length.

  $$F_{d1} = \frac{3\varepsilon_{s1} A_1}{4D_p} C_{d1} \rho_{g1} (U_{g1} - U_{s1})^2 \quad (3.20)$$

  $$F_{d2} = \frac{3\varepsilon_{s2} A_2}{4D_p} C_{d2} \rho_{g2} (U_{g2} - U_{s2})^2 \quad (3.21)$$

  The drag curve equation proposed by Clift and Guavin for calculating coefficient of drag in the two layers is given by:

  $$C_d^{\circ} = (24/Re_p)\,(1+0.15Re_p^{0.687}) + 0.42/\,(1+ 4.25 * 10^4 Re_p^{-1.16}) \quad (3.22)$$

  Where,

  $Re_p = (\rho_{air} * w_{f0} * D_p)/\mu_{air}$

  $\mu_{air} = 1.983 * 10^{-5}$ kg-m/s^2 at standard temperature 300 Kelvin.

  w_{f0}=0.06 m/s

  $D_p = 30 * 10^{-6}$ meter.

Chapter 4

Numerical Solution

4.1 Introduction

In this chapter, detailed numerical solution of the balance equations has been described. The flow parameters at the inlet of the pipe are known. Equations are solved by taking into consideration the initial values.

Dense Phase:

Table 4.1: Inlet values of the flow parameters fluidised dense phase from the data of University of Wollongong (Australia), Mallick (2009)

Test 1	ε_{s1}	ε_{g1}	U_{si} (m/s)	U_{gi} (m/s)	ρ_{gi} (kg/m^3)	ρ_{bl} (kg/m^3)	$P_{initial}$ (KPa)
Inlet x=0	0.333124	0.666876	4.707193	14.13044	3.407321	300	185.2
Test 2	ε_{s1}	ε_{g1}	U_{si} (m/s)	U_{gi} (m/s)	ρ_{gi} (kg/m^3)	ρ_{bl} (kg/m^3)	$P_{initial}$ (KPa)
Inlet x=0	0.15	0.85	0.0002	0.0083	2.47	300	106.3

Table 4.2: Inlet conditions

Initial Conditions	**Dense phase**	**Dispersed phase**
Total mass flow rate	Gas = 0.12 kg/s	Gas = 0.12 kg/s
	Solid = 19 t/h	Solid = 9 t/h
Temperature	300 K	300K

4.2 Balance Equations

Considering mass balance equation for the gas and solid phases**:**

- Mass balance equation for the gas phase in dense region:

$$\frac{d}{dx}(\rho_{g1}\varepsilon_{g1}A_1U_{g1}) = S_{mg} \quad (4.1)$$

Putting the value of S_{mg} in right hand side, we get:

$\frac{d}{dx}(\rho_{g1}\varepsilon_{g1}A_1U_{g1}) = \frac{1}{2}\rho_{g1}\varepsilon_{g1}U_{g1}S_i\frac{dh}{dx}$

$\frac{\mathrm{d}(\varepsilon_{g1}U_{g1})}{(\varepsilon_{g1}U_{g1})} = \frac{1}{2A1}\rho_{g1}S_i\frac{dh}{dx}$ *dx

Integrating both sides, we get-

$\mathrm{In}(\varepsilon_{g1}U_{g1}) = \frac{1}{2A1}\rho_{g1}S_i\frac{dh}{dx}$ *x + c

at x=0, c=1.234;

Taking antilog;

$(\varepsilon_{g1}U_{g1}) = \exp[(\frac{1}{2A1}\rho_{g1}S_i\frac{dh}{dx}$ *x) +1.234] (4.1.1)

Thus,

$\varepsilon_{g1} = \exp[(\frac{1}{2A1}\rho_{g1}S_i\frac{dh}{dx}$ *x) +1.234] /U_{g1}

- Mass balance equation for the solid phase in dense region:

$\frac{d}{dx}(\rho_{s1}\varepsilon_{s1}A_1U_{s1}) = S_{ms}$ (4.2)

We know that,

$S_{ms} = \frac{1}{2}\rho_s\varepsilon_{s1}U_{s1}S_i\frac{dh}{dx}$

Putting the value of S_{ms} in right hand side, we get:

$\frac{d}{dx}(\rho_s\varepsilon_{s1}A_1U_{s1}) = \frac{1}{2}\rho_s\varepsilon_{s1}U_{s1}S_i\frac{dh}{dx}$

$\frac{\mathrm{d}(\varepsilon_{s1}U_{s1})}{(\varepsilon_{s1}U_{s1})} = \frac{1}{2A1}S_i\frac{dh}{dx}$ * dx

Integrating both sides, we get-

$\mathrm{In}(\varepsilon_{s1}U_{s1}) = \frac{1}{2A1}S_i\frac{dh}{dx}$ *x + c

At x=0, c=1;

Taking antilog;

$(\varepsilon_{s1}U_{s1}) = \exp[(\frac{1}{2A1}S_i\frac{dh}{dx}$ *x) +1] (4.2.1)

Thus,

$\varepsilon_{s1} = \exp[(\frac{1}{2A1}S_i\frac{dh}{dx}$ *x) +1] /U_{s1}

- Mass balance equation for the gas phase in dilute region:

$\frac{d}{dx}(\rho_{g2}\varepsilon_{g2}A_2U_{g2}) = -S_{mg}$ (4.3)

We know that,

$S_{mg} = \frac{1}{2}\rho_{g1}\varepsilon_{g1}U_{g1}S_i\frac{dh}{dx}$

Putting the value of S_{mg} in above equation:

$\frac{d}{dx}(\rho_{g2}\varepsilon_{g2}A_2U_{g2}) = -\frac{1}{2}\rho_{g1}\varepsilon_{g1}U_{g1}S_i\frac{dh}{dx}$

$\rho_{g2}A_2\frac{d}{dx}(\varepsilon_{g2}U_{g2}) = -\frac{1}{2}\rho_{g1}\varepsilon_{g1}U_{g1}S_i\frac{dh}{dx}$

$\frac{d}{dx}(\varepsilon_{g2}U_{g2}) = -\frac{1}{2}\rho_{g1}(\varepsilon_{g1}U_{g1})S_i\frac{dh}{dx} / \rho_{g2}A_2$

d $(\varepsilon_{g2}U_{g2}) = -\frac{1}{2}\rho_{g1}(\varepsilon_{g1}U_{g1})S_i\frac{dh}{dx} / \rho_{g2}A_2 * dx$

Integrating both sides we get:

$(\varepsilon_{g2}U_{g2}) = -\frac{1}{2}\rho_{g1}(\varepsilon_{g1}U_{g1})S_i\frac{dh}{dx} / \rho_{g2}A_2 * x$ + c

At x = 0, c = 11.2

$(\varepsilon_{g2}U_{g2}) = -\frac{1}{2}\rho_{g1}(\varepsilon_{g1}U_{g1})S_i\frac{dh}{dx} / \rho_{g2}A_2 * x$ + 11.2 (4.3.1)

Putting the relation of $(\varepsilon_{g1}U_{g1})$ from equation (1) in the above expression, we get the equation:

$(\varepsilon_{g2}U_{g2}) = [\{-\frac{1}{2}\rho_{g1}(\exp(\frac{1}{2A1}\rho_{g1}S_i\frac{dh}{dx} * x + 1.234)S_i\frac{dh}{dx} / \rho_{g2}A_2 * x\} + 11.2]$ (4.3.2)

Thus,

$\varepsilon_{g2} = [\{-\frac{1}{2}\rho_{g1}\{ exp(\frac{1}{2A1}\rho_{g1}S_i\frac{dh}{dx} * x + 1.234)\}S_i\frac{dh}{dx} / \rho_{g2}A_2 * x\} + 11.2] / U_{g2}$

- Mass balance equation for the solid phase in dilute region:

$\frac{d}{dx}(\rho_{s2}\varepsilon_{s2}A_2U_{s2}) = -S_{ms}$ (4.4)

We know that,

$S_{ms} = \frac{1}{2}\rho_s\varepsilon_{s1}U_{s1}S_i\frac{dh}{dx}$

$\frac{d}{dx}(\rho_s\varepsilon_{s2}A_2U_{s2}) = -\frac{1}{2}\rho_s\varepsilon_{s1}U_{s1}S_i\frac{dh}{dx}$

d $(\rho_s\varepsilon_{s2}U_{s2}) = -\frac{1}{2}\rho_s\varepsilon_{s1}U_{s1}S_i\frac{dh}{dx} *$ dx

d $(\varepsilon_{s2}U_{s2}) = -\frac{1}{2A_2}(\varepsilon_{s1}U_{s1})S_i\frac{dh}{dx} *$ dx

Integrating both sides, we get:

$(\varepsilon_{s2}U_{s2})$ $= -\frac{1}{2A_2}(\varepsilon_{s1}U_{s1)}S_i\frac{dh}{dx}$ *x +c

At x= 0, c= 0

$(\varepsilon_{s2}U_{s2})$ $= -\frac{1}{2A_2}(\varepsilon_{s1}U_{s1)}S_i\frac{dh}{dx}$ *x (4.4.1)

Putting the expression of $(\varepsilon_{s1}U_{s1})$ derived from equation 2:

$(\varepsilon_{s2}U_{s2})$ $= \frac{1}{2A_2}$[exp {($\frac{1}{2A1}S_i\frac{dh}{dx}$ *x) +1}]*$S_i\frac{dh}{dx}$ *x (4.4.2)

Thus,

ε_{s2} = $\frac{1}{2A_2}$ {exp ($\frac{1}{2A1}S_i\frac{dh}{dx}$ *x) +1}*$S_i\frac{dh}{dx}$ *x] /U_{s2}

Considering the Momentum balance equations for the gas and solid phases:

- Momentum balance equation for the gas phase in dense region:

$\frac{d}{dx}(\rho_{g1}\varepsilon_{g1}A_1U_{g1}^2) = S_{mg}U_{g1} - \varepsilon_{g1}A_1\frac{dP_1}{dx} + F_{d1}$ (4.5)

Putting the values of all variables, we get:

$\frac{d}{dx}[(\varepsilon_{g1}U_{g1})A_1\,U_{g1}] = S_{mg}U_{g1} - \varepsilon_{g1}A_1\frac{dP_1}{dx} + \frac{3\varepsilon_{s1}A_1}{4D_p}C_{d1}\rho_{g1}(U_{g1}-U_{s1})^2$

$\frac{d}{dx}[(\varepsilon_{g1}U_{g1})A_1\,U_{g1}] = \frac{1}{2}\rho_{g1}(\varepsilon_{g1}U_{g1})S_i\frac{dh}{dx}*U_{g1} - \varepsilon_{g1}A_1\frac{dP_1}{dx} + \frac{3\varepsilon_{s1}A_1}{4D_p}$

$\{(24/Re_{p1})(1+0.15{Re_{p1}}^{0.687}) + 0.42/(1+4.25*10^4Re_{p1}^{-1.16})$

$*\rho_{g1}(U_{g1}-U_{s1})^2$

Using the relations obtained from equation (4.1.1) and equation (4.2.1) in the above equation to eliminate the terms of volume fractions $\varepsilon_{g1}$and ε_{s1}.

$\frac{d}{dx}$ [exp [($\frac{1}{2A1}\rho_{g1}S_i\frac{dh}{dx}$ *x) +1.234]A_1U_{g1}]= $\frac{1}{2}\rho_{g1}$ * {exp ($\frac{1}{2A1}\rho_{g1}S_i\frac{dh}{dx}$ *x)+1.234}*$S_i\frac{dh}{dx}$ *U_{g1}- $A_1\frac{dP_1}{dx}$*{exp [($\frac{1}{2A1}\rho_{g1}S_i\frac{dh}{dx}$ *x) +1.234] /U_{g1}} + $\frac{3*\{-\frac{1}{2A_2}\left[\exp\left\{\left(\frac{1}{2A_1}S_i\frac{dh}{dx}*\right)+1\right\}\right]*S_i\frac{dh}{dx}*x*A_2}{4D_p}$ * { (24/Re_{p1}) (1+0.15$Re_{p1}{}^{0.687}$) + 0.42/ (1+ 4.25 * $10^4Re_{p1}^{-1.16}$) * $\rho_{g1}(U_{g1}-U_{s1})^2/U_{s1}$ (4.5.1)

Specifying the known variables of x in terms of T1, T2, T3 and T4, we get-

T1=A_1* exp [($\frac{1}{2A1}\rho_{g1}S_i\frac{dh}{dx}$ *x) +1.234]

T2 = $\frac{1}{2}\rho_{g1}$ * {exp ($\frac{1}{2A1}\rho_{g1}S_i\frac{dh}{dx}$ *x) +1.234}*$S_i\frac{dh}{dx}$

T3= A_1* $\frac{dP_1}{dx}$* {exp [($\frac{1}{2A1}\rho_{g1}S_i\frac{dh}{dx}$ *x) +1.234]

T4= $\frac{3*\{-\frac{1}{2A_2}\left[\exp\left\{\left(\frac{1}{2A_1}S_i\frac{dh}{dx}*\right)+1\right\}\right]*S_i\frac{dh}{dx}*x*A_2}{4D_p}$* (24/$Re_{p1}$) (1+0.15$Re_{p1}{}^{0.687}$) + 0.42/ (1+ 4.25 * $10^4Re_{p1}^{-1.16}$) *ρ_{g1}

Thus the simplified coupled non-linear equation obtained is:

$\frac{d}{dx}$ (T1*U_{g1}))= T2*U_{g1} - T3/U_{g1}+ T4* $(U_{g1}-U_{s1})^2$ (4.5.2)

- Momentum balance equation for the solid phase in dense region:

$\frac{d}{dx}(\rho_s\varepsilon_{s1}A_1U_{s1}^2) = S_{ms}U_{s1} - \tau_{s1}\varepsilon_{s1}S_1 + (\varepsilon_{g2}\tau_{gsi} + \varepsilon_{s2}\tau_{ssi})\varepsilon_{s1}S_i - \varepsilon_{s1}A_1\frac{dP1}{dx} + F_{d1}$ (4.6)

Solving the equation step by step and putting the values of the complementary equations.

$$\frac{d}{dx}(\{(\varepsilon_{s1}U_{s1})A_1U_{s1}\}) = \frac{1}{2}\rho_s(\varepsilon_{s1}U_{s1})S_i\frac{dh}{dx} * U_{S1} - \left\{f_{S1}\frac{1}{2}\rho_s(U_{S1})^2\right\} * \left\{exp\left[\left(\frac{1}{2A_1}S_i\frac{dh}{dx} * X\right)+1\right]/U_{S1}\right\} * S_1 + \varepsilon_{g2}\tau_{gsi}\varepsilon_{S1}S_i + \varepsilon_{S2}\tau_{gsi}\varepsilon_{S1}S_i - \varepsilon_{S1}A_1\frac{dP1}{dx} + \frac{3\varepsilon_{S1}A_1}{4D_P}\left\{\left(\frac{24}{Re_{P1}}\right)\left(1+0.15{Re_{p1}}^{0.687}\right)\right\} + \frac{0.42}{\left(1+4.24*10^4\,{Re_{p1}}^{-1.16}\right)} * \rho_{g1}\left(U_{g1}-U_{s1}\right)^2$$

$\frac{d}{dx}$ ($A_1 * \exp\{\left(\frac{1}{2A_1}S_i\frac{dh}{dx} *$ $\frac{1}{2}\rho_s$ *exp{$\left(\frac{1}{2A1}\mathrm{S_i}\frac{\mathrm{dh}}{\mathrm{dx}} * \mathrm{x}\right)$+1}*$S_i * \frac{dh}{dx}$*$U_{s1}$-{$f_{s1}\frac{1}{2}\rho_s$}* {exp $x\big) + 1\} * U_{s1}$) = [($\frac{1}{2A1}S_i\frac{dh}{dx}$ *x) +1]* U_{s1} + {[{$\frac{1}{2}\rho_{g1}$(exp ($\frac{1}{2A1}\rho_{g1}S_i\frac{dh}{dx}$ * x + 1.234)$S_i\frac{dh}{dx}$ / $\rho_{g2}A_2$ *x} + 11.2]*{ f_{gi}*$\frac{1}{2}\rho_{g2}$* exp [($\frac{1}{2A1}\rho_{g1}S_i\frac{dh}{dx}$ *x)+1.234] * exp [($\frac{1}{2A1}S_i\frac{dh}{dx}$ *x) +1]* (U_{g2} − U_{s1})^2/$U_{g2}U_{s1}$+[− $\frac{1}{2A_2}$ {exp ($\frac{1}{2A1}S_i\frac{dh}{dx}$ *x) +1}* $S_i\frac{dh}{dx}$ *x] * $f_{si}\frac{1}{2}\rho_s$*exp[($\frac{1}{2A1}S_i\frac{dh}{dx}$*x)+1 * S_i*{($U_{s2}-U_{s1}$)^2/$U_{s2}U_{s1}$}- exp [($\frac{1}{2A1}S_i\frac{dh}{dx}$ *x) +1]*$A_1\frac{dP1}{dx}$ + $\frac{3*\{-\frac{1}{2A_2}\left[\exp\left\{\left(\frac{1}{2A_1}S_i\frac{dh}{dx} *\right)+1\right\}\right]*S_i\frac{dh}{dx}*x*A_2}{4D_p}$ *{(24/Re_{p1}) * (1+0.15${Re_{p1}}^{0.687}$)} + 0.42/ (1+ 4.25 * 10^4 $Re_{p1}^{-1.16}$) *$\rho_{g1}(U_{g1}-U_{s1})^2/U_{s1}$

(4.6.1)

Specifying the known variables of x in terms of T1, T2, T3, T4, T5, and T6 we get:

$$T1 = A_1 * \exp\left[\left(\frac{1}{2A1} S_i \frac{dh}{dx} \ *x\right) +1\right]$$

$$T2 = \frac{1}{2}\rho_s * \exp\left[\left(\frac{1}{2A1} S_i \frac{dh}{dx} \ *x\right) +1\right] * S_i * \frac{dh}{dx}$$

$$T3 = \left\{f_{s1} \frac{1}{2}\rho_s\right\} * \{\exp\left[\left(\frac{1}{2A1} S_i \frac{dh}{dx} \ *x\right) +1\right]$$

$$T4 = \{[\{-\frac{1}{2}\rho_{g1}(\exp\left(\frac{1}{2A1}\rho_{g1} S_i \frac{dh}{dx} \ * x + 1.234\right) S_i \frac{dh}{dx} / \rho_{g2} A_2 *x\} + 11.2] * \{ f_{gi} * \frac{1}{2}\rho_{g2} * \exp\left[\left(\frac{1}{2A1}\rho_{g1} S_i \frac{dh}{dx} \ *x\right) +1.234\right] * \exp\left[\left(\frac{1}{2A1} S_i \frac{dh}{dx} \ *x\right) +1\right]$$

$$T5 = \frac{1}{2A_2}\{\exp\left(\frac{1}{2A1} S_i \frac{dh}{dx} \ *x\right) +1\} * S_i \frac{dh}{dx} *x] * f_{si} \frac{1}{2}\rho_s * \exp[(\frac{1}{2A1} S_i \frac{dh}{dx} \ * x) +1] * S_i$$

$$T6 = A_1 * \exp\left[\left(\frac{1}{2A1}\rho_{g1} S_i \frac{dh}{dx} \ *x\right) +1\right] * \frac{dP_1}{dx} + \frac{3*\{-\frac{1}{2A_2}\left[\exp\left\{\left(\frac{1}{2A_1} S_i \frac{dh}{dx} \ *\right)+1\right\}\right] * S_i \frac{dh}{dx} *x*A_2}{4D_p} * \{(24/Re_{p1})\ (1+0.15 {Re_{p1}}^{0.687})\} + 0.42/\ (1+ 4.25 * 10^4 \ \ Re_{p1}^{-1.16}\ ) * \rho_{g1}$$

Thus the simplified coupled non-linear equation obtained is:

$$\frac{d}{dx}\ (T_1 * U_{s1})) = = T2 * U_{s1} - T3 * U_{s1} - T4 * (\frac{U_{g2}}{U_{s1}} + \frac{U_{s1}}{U_{g2}} - 2) - T5 * (\frac{U_{s2}}{U_{s1}} + \frac{U_{s1}}{U_{s2}} - 2) - T6 * (\frac{U_{G1}^2}{U_{S1}} + U_{S1} - 2\ U_{g1}) \quad (4.6.2)$$

- Momentum balance equation for the gas phase in dilute region:

$$\frac{d}{dx}\left(\rho_{g2}\varepsilon_{g2}A_2 U_{g2}^2\right) = -S_{mg}U_{g1} - \tau_{g2}\varepsilon_{g2}S_2 - \varepsilon_{s1}\varepsilon_{g2}\tau_{gsi}S_i - \varepsilon_{g2}A_2\frac{dP_2}{dx} - F_{d2} \quad (4.7)$$

Solving the equation step by step and putting the values of the complementary equations.

$\frac{d}{dx}\left[\rho_{g2}\left(U_{g2}\varepsilon_{g2}\right)A_2 * U_{g2}\right] =$ $-\frac{1}{2}\rho_{g1}(\varepsilon_{g1}U_{g1})S_i\frac{dh}{dx} * U_{g1} - f_{g2} * \frac{1}{2}\rho_{g2} *$
$[\{-\frac{1}{2}\rho_{g1}(\exp\left(\frac{1}{2A1}\rho_{g1}S_i\frac{dh}{dx} * \mathrm{x} + 1.234\right)S_i * \frac{dh}{dx} /$
$\rho_{g2}A_2 * \mathrm{x}\} + 11.2] * S_2 * U_{g2} - \exp[(\frac{1}{2A1}S_i\frac{dh}{dx} * \mathrm{x}) + 1] *$
$[\{-\frac{1}{2}\rho_{g1}(\exp\left(\frac{1}{2A1}\rho_{g1}S_i\frac{dh}{dx} * \mathrm{x} + 1.234\right)S_i\frac{dh}{dx} /$
$\rho_{g2}A_2 * x\} + 11.2] * * f_{gi} * \frac{1}{2} * \rho_{g2} * S_i *$
$(U_{g2} - U_{s1})^2 / U_{g2}U_{s1} - \mathrm{A}_2 * \frac{\mathrm{dP}_2}{\mathrm{dx}} * [[\{-$
$\frac{1}{2}\rho_{g1} * (\exp\left(\frac{1}{2A1}\rho_{g1}S_i\frac{dh}{dx} * \mathrm{x} + 1.234\right)S_i *$
$\frac{dh}{dx}\rho_{g2}A_2 * \mathrm{x}\} + 11.2] / U_{g2} - \frac{3\varepsilon_{s2}A_2}{4D_p}C_{d2}\rho_{g2}(U_{g2} - U_{s2})^2$

$\frac{d}{dx}[\rho_{g2}A_2 *$ $-\frac{1}{2}\rho_{g1} * (\exp[\left(\frac{1}{2A1}\rho_{g1}S_i\frac{dh}{dx} * \mathrm{x}\right) + 1.234] * S_i\frac{dh}{dx} * U_{g1} -$
$\{-\frac{1}{2}\rho_{g1}(\exp(\frac{1}{2A1}\rho_{g1}S_i\frac{dh}{dx} * \mathrm{x} +$ $f_{g2} * \frac{1}{2}\rho_{g2} * [\{\frac{1}{2}\rho_{g1}(\exp(\frac{1}{2A1}\rho_{g1}S_i\frac{dh}{dx} * \mathrm{x} + 1.234)S_i\frac{dh}{dx} /$
$1.234)S_i\frac{dh}{dx} / \rho_{g2}A_2 * x\} + 11.2)\} *$ $\rho_{g2}A_2 * \mathrm{x}\} + 11.2] * S_2 * U_{g2} - \exp$
$U_{g2}] =$ $[(\frac{1}{2A1}S_i\frac{dh}{dx} * \mathrm{x}) + 1] * [\{-\frac{1}{2}\rho_{g1} * [\exp(\frac{1}{2A1}\rho_{g1}S_i\frac{dh}{dx} * \mathrm{x} +$
$1.234)]S_i\frac{dh}{dx}\rho_{g2}A_2 * \mathrm{x}\} + 11.2] * f_{gi} * \frac{1}{2} * \rho_{g2} * S_i * (\frac{U_{g2}}{U_{s1}} + \frac{U_{s1}}{U_{g2}} -$
$2) - \mathrm{A}_2 * \frac{\mathrm{dP}_2}{\mathrm{dx}} [\{-\frac{1}{2}\rho_{g1} * (\exp(\exp\left(\frac{1}{2A1}\rho_{g1}S_i\frac{dh}{dx} * \mathrm{x} +$
$1.234\right)S_i\frac{dh}{dx}\rho_{g2}A_2 * \mathrm{x}\} + 11.2] * f_{gi} * \frac{1}{2} * \rho_{g2} * S_i * (\frac{U_{g2}}{U_{s1}} + \frac{U_{s1}}{U_{g2}} -$
$2) - \mathrm{A}_2 * \frac{\mathrm{dP}_2}{\mathrm{dx}} [\{-\frac{1}{2}\rho_{g1} * (\exp(\mathrm{xp}\left(\frac{1}{2A1}\rho_{g1}S_i\frac{dh}{dx} * \mathrm{x} +$
$1.234\right) * S_i * \frac{dh}{dx}\rho_{g2}A_2 * \mathrm{x}\} + 11.2] / U_{g2} -$
$\frac{3 * \{-\frac{1}{2A_2}\left[\exp\left\{\left(\frac{1}{2A_1}S_i\frac{dh}{dx} *\right) + 1\right\}\right] * S_i\frac{dh}{dx} * \mathrm{x} * A_2}{4D_p}$
$* \left\{\left(\frac{24}{Re_{p1}}\right)\left(1 + 0.15Re_{p1}^{0.687}\right)\right\} + \frac{0.42}{\mathrm{Re_{p2}}}$
$\left(1 + 4.25 * 10^4 Re_{p2}^{-1.16}\right) * \rho_{g2} * (\frac{U_{g2}^2}{U_{s2}} + U_{s2} - 2U_{g2}). =$

$\frac{d}{dx}[\rho_{g2}A_2\{-\frac{1}{2}\rho_{g1}(\exp((\frac{1}{2A1}\rho_{g1}S_i\frac{dh}{dx} * x + 1.234)S_i\frac{dh}{dx} / \rho_{g2}A_2 *x\} + 11.2)\} * U_{g2}] =$

$-\frac{1}{2}\rho_{g1}(\exp\left(\frac{1}{2A1}\rho_{g1}S_i\frac{dh}{dx} * x\right)+1.234) * S_i\frac{dh}{dx} * U_{g1} - f_{g2} * \frac{1}{2}\rho_{g2} * [\{\frac{1}{2}\rho_{g1}(\exp((\frac{1}{2A1}\rho_{g1}S_i\frac{dh}{dx} * x + 1.234)S_i\frac{dh}{dx} / \rho_{g2}A_2 * x + 11.2] * S_2 * U_{g2} - \exp[(\frac{1}{2A1}S_i\frac{dh}{dx} * x) + 1] * [\{-\frac{1}{2}\rho_{g1} * \exp((\frac{1}{2A1}\rho_{g1}S_i\frac{dh}{dx} * x + 1.234)S_i\frac{dh}{dx} / \rho_{g2}A_2 * x\} + 11.2] * f_{gi}\frac{1}{2} * \rho_{g2} * S_i * (\frac{U_{g2}}{U_{s1}} + \frac{U_{s1}}{U_{g2}} - 2) - A_2 * \frac{dP_2}{dx} * [\{\frac{1}{2}\rho_{g1}(\exp\left(\frac{1}{2A1}\rho_{g1}S_i\frac{dh}{dx} * x + 1.234\right)S_i * \frac{dh}{dx}\rho_{g2}A_2 * x\} + 11.2] / U_{g2} - \frac{3 * \{-\frac{1}{2A_2}\left[\exp\left\{\left(\frac{1}{2A_1}S_i\frac{dh}{dx} *\right) + 1\right\}\right] * S_i\frac{dh}{dx} * x * A_2}{4D_p} * \left\{\left(\frac{24}{Re_{p1}}\right)\left(1 + 0.15{Re_{p1}}^{0.687}\right)\right\} + \frac{0.42}{Re_{p2}}\left(1 + 4.25 * 10^4 Re_{p2}^{-1.16}\right) * \rho_{g2} * (\frac{U_{g2}^2}{U_{s2}} + U_{s2} - 2U_{g2}).$ (4.7.1)

Specifying the known variables of x in terms of T1, T2, T3, T4, T5, and T6 we get:

T1= $\rho_{g2} * A_2 * \{-\frac{1}{2}\rho_{g1}(\exp(\frac{1}{2A1}\rho_{g1}S_i\frac{dh}{dx} * x + 1.234)S_i\frac{dh}{dx} / \rho_{g2}A_2 * x\} + 11.2)\}$

T2 = $-\frac{1}{2}\rho_{g1} * (\exp[(\frac{1}{2A1}\rho_{g1}S_i\frac{dh}{dx} * x) + 1.234]) * S_i\frac{dh}{dx}$

T3 = $f_{g2} * \frac{1}{2}\rho_{g2} * [\exp\left(\frac{1}{2A1}\rho_{g1}S_i\frac{dh}{dx} * x + 1.234\right)] * \frac{dh}{dx} * \rho_{g2}A_2 * x\} + 11.2] * S_2$

T4= $\exp[(\frac{1}{2A1}S_i\frac{dh}{dx} * x) + 1] * [\{-\frac{1}{2}\rho_{g1} * (\exp(\frac{1}{2A1}\rho_{g1}S_i\frac{dh}{dx} * x + 1.234)S_i\frac{dh}{dx} / \rho_{g2}A_2 * x\} + 11.2] * f_{gi} * \frac{1}{2} * \rho_{g2} * S_i$

T5 = $-A_2 * \frac{dP_2}{dx} * [\{-\frac{1}{2}\rho_{g1} * (\exp\left(\frac{1}{2A1}\rho_{g1}S_i\frac{dh}{dx} * x + 1.234\right)S_i\frac{dh}{dx}\rho_{g2}A_2 * x\} + 11.2]$

$$T6 = \frac{3 * \{-\frac{1}{2A_2}\left[\exp\left\{\left(\frac{1}{2A_1}S_i\frac{dh}{dx} *\right)+1\right\}\right] * S_i\frac{dh}{dx} * x * A_2}{4D_p} * \left\{\left(\frac{24}{Re_{p1}}\right)\left(1+0.15{Re_{p1}}^{0.687}\right)\right\} + \frac{0.42}{\mathrm{Re_{p2}}}\left(1+ 4.25 * 10^4 Re_{p2}^{-1.16}\right) * \rho_{g2}$$

Thus the simplified coupled non-linear equation obtained is:

$$\frac{d}{dx}(T_1 * U_{g2}))= T2*U_{g1} - T3/U_{g2} - T4*(\frac{U_{g2}}{U_{s1}} + \frac{U_{s1}}{U_{g2}} - 2) - T5/U_{g2} - T6*(\frac{U_{G1}^2}{U_{S1}} + U_{S1} - 2\ U_{g1}) \quad (4.7.2)$$

- Momentum balance equation for the solid phase in dilute region:

$$\frac{d}{dx}(\rho_s\varepsilon_{s2}A_2U_{s2}^2) = -S_{ms}U_{s1} - \tau_{s1}\varepsilon_{s1}S_1 - \varepsilon_{s2}\tau_{ssi}\varepsilon_{s1}S_i - \varepsilon_{s2}A_2\frac{dP_2}{dx} - F_{d2}$$

$$\frac{d}{dx}(\rho_s(\varepsilon_{s2}U_{s2})A_2U_{s2}) = = -\frac{d}{dx}(\rho_{s1}\varepsilon_{s1}A_1U_{s1})*U_{s1} - f_{s1}\frac{1}{2}\rho_s*\exp[(\frac{1}{2A1}S_i\frac{dh}{dx} *x) +1]*S_1 *U_{s1} - \frac{1}{2A_2}\{\exp(\frac{1}{2A1}S_i\frac{dh}{dx} *x) +1\}*S_i\frac{dh}{dx} *x]*f_{si}\frac{1}{2}\rho_s** \exp[\left(\frac{1}{2A1}S_i\frac{dh}{dx} * x\right)+1]* S_i*((U_{s2} - U_{s1})^2/U_{s2}U_{s1} - \{-\frac{1}{2A_2}[\exp\{(\frac{1}{2A1}S_i\frac{dh}{dx} *x) +1\}]*S_i\frac{dh}{dx} *x\}*A_2 * \frac{dP_2}{dx}/U_{s2} - \frac{3\varepsilon_{s2}A_2}{4D_p}C_{d2}\rho_{g2}(U_{g2} - U_{s2})^2 \quad (4.8)$$

$$\frac{d}{dx}(\rho_s\{-\frac{1}{2A_2} *\exp\{(\frac{1}{2A1}S_i\frac{dh}{dx} * x)+1\}*S_i\frac{dh}{dx}\} ** A_2U_{s2}) = -\frac{d}{dx}(\rho_{s1}\{-\frac{1}{2A1}S_i\frac{dh}{dx} *x) +1\}*A_1)*U_{s1} - f_{s1}\frac{1}{2}\rho_s* \exp[(\frac{1}{2A1}S_i\frac{dh}{dx} *x) +1]*S_1 *U_{s1} - \frac{1}{2A_2}\{\exp(\frac{1}{2A1}S_i\frac{dh}{dx} *x) +1\}*S_i\frac{dh}{dx} *x]*f_{si}\frac{1}{2}\rho_s*\exp[\left(\frac{1}{2A1}S_i\frac{dh}{dx} * x\right)+1]* S_i*(\frac{U_{s2}}{U_{s1}} + \frac{U_{s1}}{U_{s2}} - 2) - \{-\frac{1}{2A_2}[\exp\{(\frac{1}{2A1}S_i\frac{dh}{dx} *x) +1\}]*S_i\frac{dh}{dx} *x\}*A_2 * \frac{dP_2}{dx}/U_{s2} -$$

$$\frac{3 * \{-\frac{1}{2A_2}\left[\exp\left\{\left(\frac{1}{2A_1} S_i \frac{dh}{dx} \ *\right) + 1\right\}\right] * S_i \frac{dh}{dx} \ * \mathrm{x} * A_2}{4D_p}$$

$$* \left\{\left(\frac{24}{Re_{p1}}\right)\left(1 + 0.15 {Re_{p1}}^{0.687}\right)\right\} + \frac{0.42}{\mathrm{Re_{p2}}}\left(1 + \ 4.25 \ * \right.$$

$$\left. 10^4 Re_{p2}^{-1.16}\right) * \rho_{g2} * \left(\frac{U_{g2}^2}{U_{s2}} + U_{s2} - 2U_{g2}\right)$$

(4.8.1)

Specifying the known variables of x in terms of T1, T2, T3, T4 and T5 we get:

T1 $= \rho_s\{-\frac{1}{2A_2} * \exp\{(\frac{1}{2A1} S_i \frac{dh}{dx} \ * \mathrm{x}) \ + 1\} * S_i \frac{dh}{dx}\} * A_2$

T2 = $-\frac{d}{dx}(\rho_{s1} * \exp[(\frac{1}{2A1} S_i \frac{dh}{dx} \ * \mathrm{x}) + 1] * A_1) *$

T3 = $\frac{1}{2A_2}\{\exp(\frac{1}{2A1} S_i \frac{dh}{dx} \ * \mathrm{x}) + 1\} * S_i \frac{dh}{dx} * \mathrm{x}] * f_{si} \frac{1}{2} * \rho_s * \ \mathbf{e}\exp\left[\left(\frac{1}{2A1} S_i \frac{dh}{dx} \ * \mathrm{x}\right) + 1\right] S_i$

T4 = $-\frac{1}{2A_2}[\exp\{(\frac{1}{2A1} S_i \frac{dh}{dx} \ * \mathrm{x}) + 1\}] * S_i \frac{dh}{dx} * \mathrm{x}\} * \mathrm{A}_2$

T5 = $\frac{3 * \{-\frac{1}{2A_2}\left[\exp\left\{\left(\frac{1}{2A_1} S_i \frac{dh}{dx} \ *\right) + 1\right\}\right] * S_i \frac{dh}{dx} \ * \mathrm{x} * A_2}{4D_p}$

$$* \left\{\left(\frac{24}{Re_{p1}}\right)\left(1 + 0.15 {Re_{p1}}^{0.687}\right)\right\} + \frac{0.42}{\mathrm{Re_{p2}}}\left(1 + \ 4.25 \ * \ 10^4 Re_{p2}^{-1.16}\right)$$

$$* \rho_{g2}$$

Thus the simplified coupled non-linear equation obtained is:

$\frac{d}{dx}\ (T_1 * U_{s2}))$= T2*$U_{s1}$ – T3*$(\frac{U_{g2}}{U_{s1}} + \frac{U_{s1}}{U_{g2}} - 2)$ – T4/U_{s2} –T5*$(\frac{U_{G1}^2}{U_{S1}} + U_{S1} - 2\ U_{g1})$ (4.8.2)

- Thus, the four evolution equations derived from the simplifications of above eight balance equations are

$$\frac{d}{dx}(T_1 * U_{g1}) = \text{T2}*U_{g1} - \text{T3}/U_{g1} + \text{T4}*\left(U_{g1} - U_{s1}\right)^2 \quad (4.5.2)$$

$$\frac{d}{dx}(T_1 * U_{s1})) = \text{T2}*U_{s1} - \text{T3}*U_{s1} - \text{T4}*\left(\frac{U_{g2}}{U_{s1}} + \frac{U_{s1}}{U_{g2}} - 2\right) - \text{T5}*\left(\frac{U_{s2}}{U_{s1}} + \frac{U_{s1}}{U_{s2}} - 2\right) - \text{T6}*\left(\frac{U_{G1}^2}{U_{S1}} + U_{S1} - 2\,U_{g1}\right) \quad (4.6.2)$$

$$\frac{d}{dx}(T_1 * U_{g2})) = \text{T2}*U_{g1} - \text{T3}/U_{g2} - \text{T4}*\left(\frac{U_{g2}}{U_{s1}} + \frac{U_{s1}}{U_{g2}} - 2\right) - \text{T5}/U_{g2} - \text{T6}*\left(\frac{U_{G1}^2}{U_{S1}} + U_{S1} - 2\,U_{g1}\right) \quad (4.7.2)$$

$$\frac{d}{dx}(T_1 * U_{s2})) = \text{T2}*U_{s1} - \text{T3}*\left(\frac{U_{g2}}{U_{s1}} + \frac{U_{s1}}{U_{g2}} - 2\right) - \text{T4}/U_{s2} - \text{T5}*\left(\frac{U_{G1}^2}{U_{S1}} + U_{S1} - 2\,U_{g1}\right) \quad (4.8.2)$$

The MATLAB script for determining the constant terms in evolution equations (T1, T2, T3, T4, T5, T6) are given in Appendix A.

Chapter 5

Results and Discussions

5.1 Introduction

The inlet flow conditions obtained from the experiments were used as a basis for calculating the flow variables at the different length segments of the pipeline.

The set of first order nonlinear ordinary differential equations comprises of 8 equations and 8unknowns U_{s1},U_{g1}, ε_{s1}, ε_{g1},U_{s2},U_{g2}, ε_{s2}, ε_{g2}

Numerical solution of these equations involve the solution of evolution equations in MATLAB with the initial conditions i.e. (x=0) to obtain the values of variables at every segment of pipeline and a MATLAB program for solving the flow equations using fourth-order Runge- Kutta method. Numerically calculated values of parameters acquired towards the end of the first pipe section serve as the initial conditions for the progressive section. This practice has been taken after up to the exit point of the pipeline. Values of the parameters U_s, U_g, ε_s, ε_g and $\frac{U_s}{U_g}$ for both dense phase and dispersed phase were determined at the initial and final point of each section neglecting the variation of cross section along the length and from this, outcomes corresponding to the midpoint values (at x = 3.26, 24.62, 60.84, 81.31, 98.78, 129 m and 150.08m) were fetched. The results (variation ofU_s,U_g, ε_s, ε_g and $\frac{U_s}{U_g}$ along the length of pipeline (from x = 3.26 to 150.08 m) are provided in the following Figures. 5.1 to 5.5.

Figures from 5.1 to 5.3 show variation of U_s, U_g and $\frac{U_s}{U_g}$ along the length of the pipeline. Each figure shows two trend lines corresponding to two different mass flow rates: ($\mathrm{m_{s1}} = \frac{19\mathrm{t}}{\mathrm{h}}$, $\mathrm{m_{a1}} = 0.12\mathrm{kg/s}$) and ($\mathrm{m_{s2}} = \frac{9\mathrm{t}}{\mathrm{h}}$, $\mathrm{m_{a2}} = 0.12\mathrm{kg/s}$).

As can be seen from figure 5.1, the actual flow velocity of air increases along the length of the pipeline. In addition to it, there is mass transfer from upper layer to lower layer tending to dilute the bottom layer. The effect of the larger mass flow rate of lower layer is to dilute the layer and to transport the solid particles into the top layer which may be attributed to the fact that for the isothermal flow of the gas solids mixture, the gas density declines along the length of the pipeline due to decreasing pressure. Therefore the gas velocities in both the layers must increase correspondingly for satisfying the continuity law.

As a consequence the height of the dense layer decreases and solids particles get suspended in air in the dispersed phase which causes variation in the cross sectional area. This also causes change in the gas velocities of both the dense and dilute layers.

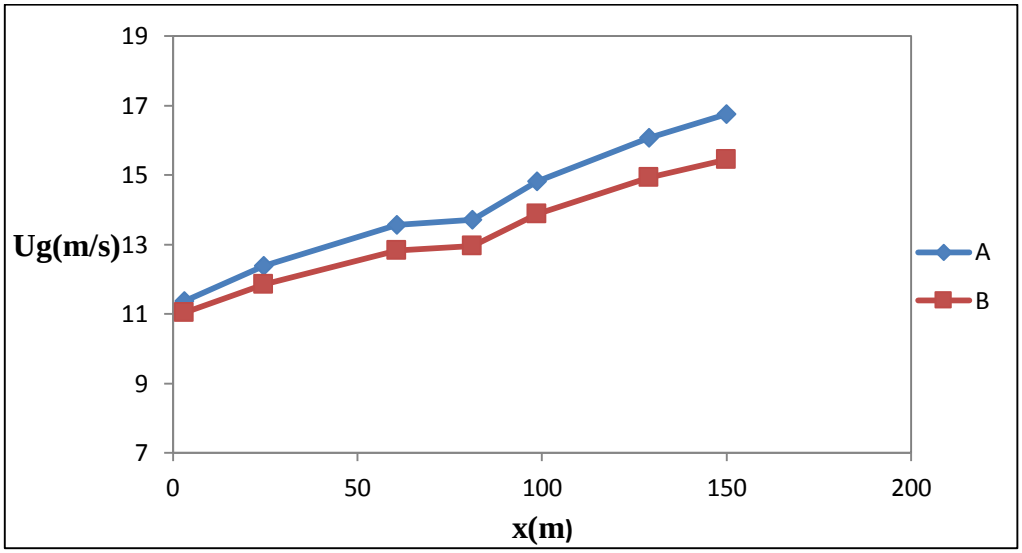

A:	ρ_b=300 kg/ m^3 ; m_s =19t/h, ma = 0.12kg/s (Dense Phase)
B:	ρ_b =300 kg/ m^3 ; m_s =9t/h, m_a = 0.12kg/s (Dilute Phase)

Figure 5.1: Variation of actual gas velocity in dense and dilute layers for the same bulk density through pipeline (69 mm I.D X160 m long pipe)

In figure 5.2, the solid particles velocity also increases along the length of the pipeline. Higher gas flow rates bring about bigger addition in the estimation of the particle velocity. So with the increase in the expansion of actual gas velocity, the particles velocities also increase along the length of the flow. Thus along the length of the pipeline the solid particles gain velocity and the solids velocity of both the layers keeps increasing.

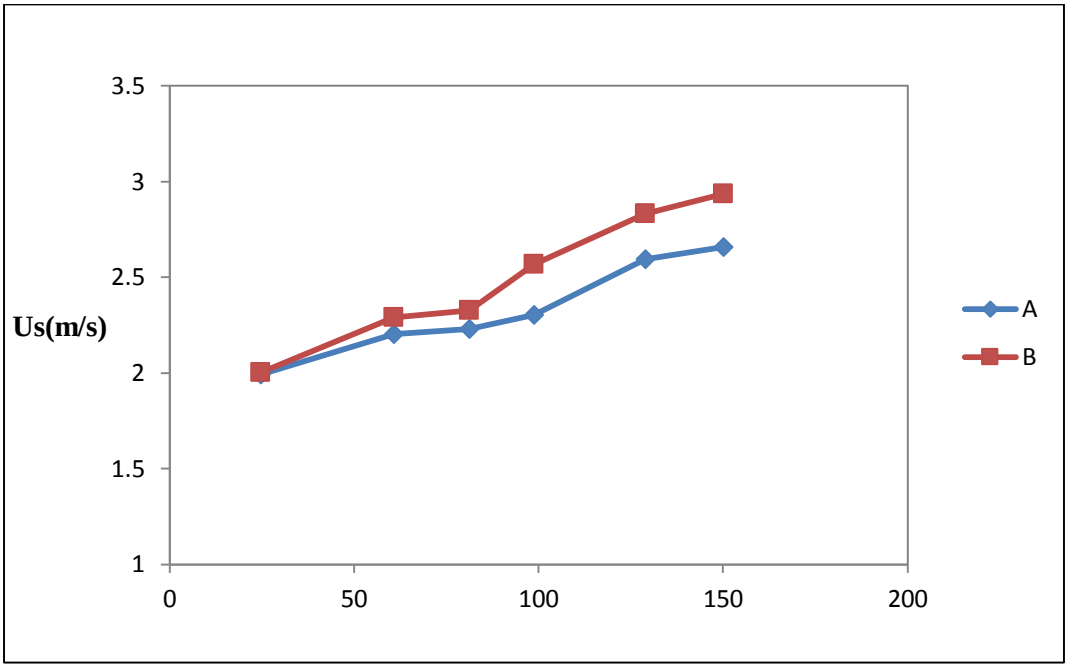

A:	ρ_b=300 kg/ m^3 ; m_s =19t/h, ma= 0.12kg/s (Dense Phase)
B:	ρ_b =300 kg/ m^3 ; m_s =9t/h, m_a = 0.12kg/s (Dilute Phase)

Figure 5.2: Variation of solids velocity in dense and dilute layers for the same bulk density through pipeline (69 mm I.D X160 m long pipe)

Figure 5.3 shows the ratios of proportion of particles to gas speeds. The ratio increment towards flow direction showing that the increment in gas velocity (because of gas expansion) is all the more ruling over the corresponding rise in speed of particles. There is a bigger slip between the gas and solids stages in flow direction.

High gas velocity promotes the flow of solids particles in both the layers. Thus, it can be concluded that the gas velocity is the ruling factor over the solids velocity.

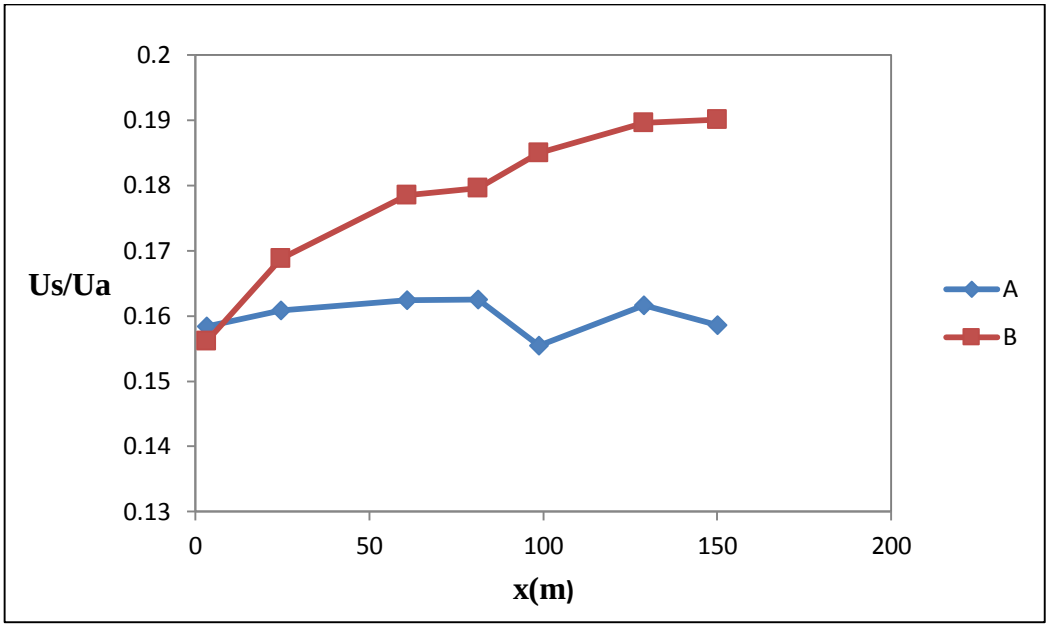

A: ρ_b=300 kg/ m^3 ; m_s =19t/h, ma= 0.12kg/s (Dense Phase)

B: ρ_b =300 kg/ m^3 ; m_s =9t/h, m_a = 0.12kg/s (Dilute Phase)

Figure 5.3: Variation of solid to air velocity ratio in dense and dilute layers for the same bulk density through pipeline (69 mm I.D X160 m long pipe)

Figure 5.4 and Figure 5.5 show the variation of solid and air volume fractions (ε_s and ε_a) along the length of the pipeline for the mass flow rates: ($m_{s1} = \frac{19t}{h}$, $m_{a1} = 0.12kg/s$) and ($m_{s2} = \frac{9t}{h}$, $m_{a2} = 0.12kg/s$)

Volumetric flow rate of air is written as:

$$V_a = \frac{m_a RT}{P} \tag{5.1}$$

And Solids volumetric flow rate is written as:

$$V_s = \frac{m_s}{\rho_{bl}} \tag{5.2}$$

Using equations (5.1) and (5.2) in equation (5.3), solids volume fraction and volume fraction of air can be calculated.

$$\varepsilon_a = \frac{V_a}{V_s + V_a} \text{ And } \varepsilon_s = 1 - \varepsilon_a \tag{5.3}$$

As shown in figure 5.4,the volume fraction of gas increases along the length of the pipeline due to continuous expansion of the gases as the flow proceeds from the beginning up to the end of the pipeline though the mass flow rates of solids remain constant under steady state conditions.

In other words, as the flow begins the gas expands, the material becomes more aerated. As a result, void fraction increases and in an ultimate condition, the dense flow is converted into dilute flow, i.e. fluidization takes place.

Results from simulation showed that the volume fraction of gas keep increasing from inlet to exit of pipeline.

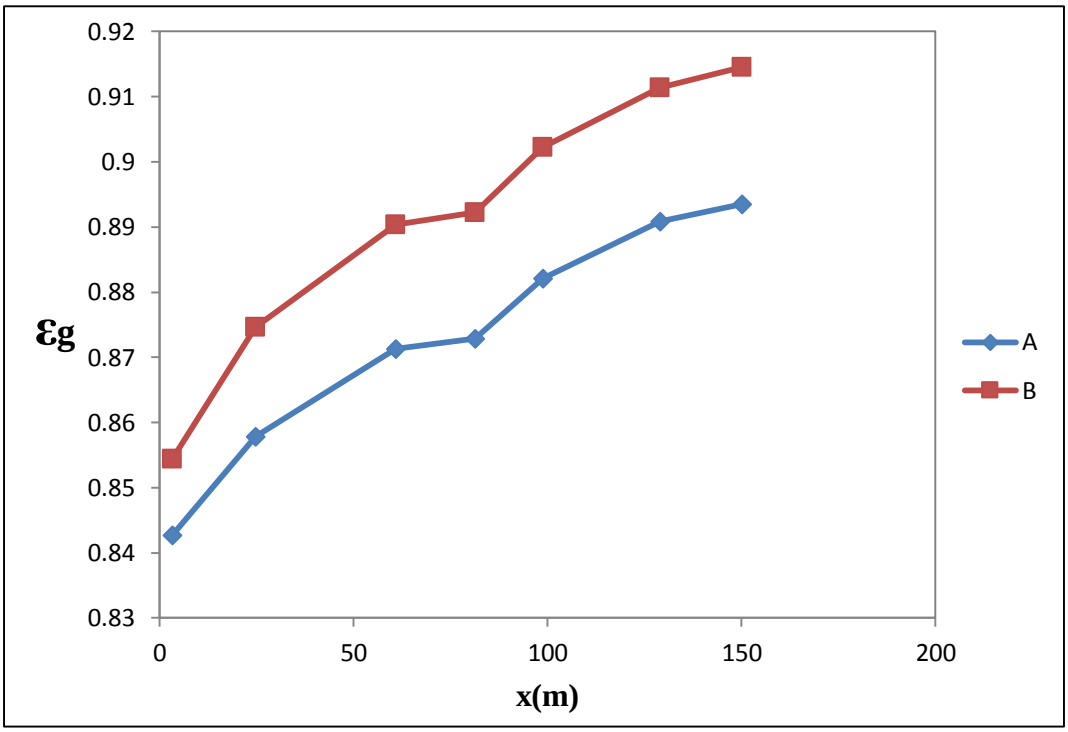

A: ρ_b=300 kg/ m^3 ; m_s =19t/h, m_a = 0.12kg/s (Dense Phase)

B: ρ_b =300 kg/ m^3 ; m_s =9t/h, m_a = 0.12kg/s (Dilute Phase)

Figure 5.4: Variation of gas volume fraction in dense and dilute layers for the same bulk density through pipeline (69 mm I.D X160 m long pipe)

So, as the volume fraction of gases increase along the length of the pipeline due to gas expansion, the volume fraction of the solids decrease correspondingly from inlet to exit of the pipeline as shown in figure 5.5.

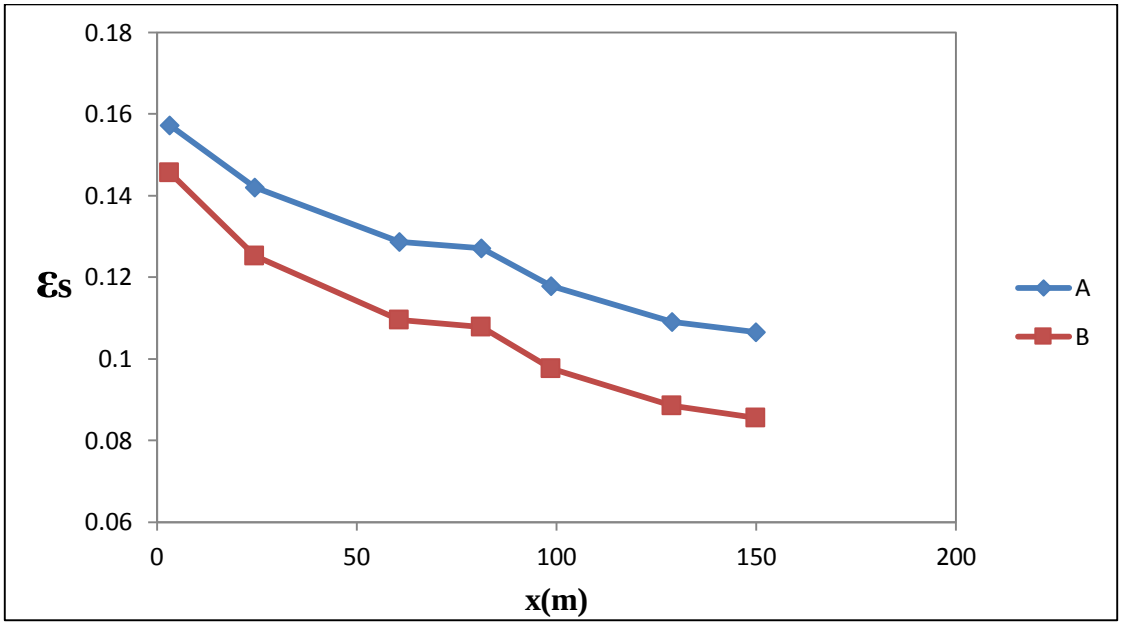

A: ρ_b=300 kg/ m^3 ; m_s =19t/h, ma= 0.12kg/s (Dense Phase)

B: ρ_b =300 kg/ m^3 ; m_s =9t/h, m_a = 0.12kg/s (Dilute Phase)

Figure 5.5: Variation of solid volume fraction in dense and dilute layers for the same bulk density along the flow direction

Chapter 6

Conclusion

6.1 Conclusion

A fluidised dense layer model has been developed based on the fundamental equations of physics to assess the behaviour of flow parameters along the length of the pipeline. The non-linear coupled equations were solved in MATLAB and the behaviour of the model in terms of solid particles velocity, actual gas velocity and volume fractions of solids and gases was examined.

The conclusions ventured are:

1. For the isothermal flow of the gas solids mixture, the density of gas declines along the length of the pipeline due to falling pressure. Therefore, the gas velocities in both the layers rise correspondingly satisfying the continuity law.
2. High gas velocity promotes the flow of solids particles in both the layers; dense as well as dilute. Thus, it can be concluded that the gas velocity is predominating over the solids velocity.
3. As the flow proceeds, the gas expands, the material becomes more aerated and the volume fraction of gas increases as the void area increases. Correspondingly, the volume fraction of solids falls.
4. Along the length of the pipe, the flow is becoming dilute.

6.2 Future scope of work

1. The model can be developed as a pure mathematical model.
2. The model can be used to predict pressure drop and to compare with available experimental data for a different pipeline configuration. The variation of pressure drop with change in pipe diameter and pipeline length can be analysed under different flow conditions to test the behaviour of model under different conditions.

References

Baerns, M., 1966. Effect of interparticle adhesive forces on fluidization of fine particles. Industrial & Engineering Chemistry Fundamentals, 5(4), pp.508-516.

Behera, N., Agarwal, V.K., Jones, M. and Williams, K.C., 2013. Modeling and Analysis of Solids Friction Factor for Fluidized Dense Phase Pneumatic Conveying of Powders. Particulate Science and Technology, 31(2), pp.136-146.

Dormand, J.R. and Prince, P.J., 1980. A family of embedded Runge-Kutta formulae. Journal of computational and applied mathematics, 6(1), pp.19-26.

Fargette, C., Jones, M.G. and Nussbaum, G., 1996, December. Bench scale tests for the assessment of pneumatic conveying behavior of powders. In 54 th Electric Furnace Conference (pp. 195-205).

Hong, J. and Tomita, Y., 1996. Analysis of high density gas-solids stratified pipe flow. International Journal of Multiphase Flow, 1001(22), p.121.

Houcque, D., 2008. Applications of MATLAB: Ordinary differential equations (ODE). Robert R. McCormick School of Engineering and Applied Science-Northwestern University, Evanston.

Huang, W., X. Gong, X. Guo, Z. Dai, H. Liu, Z. Cao, and C. Wang.2009. Study of the pressure drop of dense phase gas–solid flow through nozzle. Powder Technology 189: 82-86.

Jones, M. G., and K. C. Williams. 2003. Solids friction factor for fluidized dense-phase conveying. Particulate Science and Technology 21: 45–56.

Klinzing, G. E., C. A. Myler, A. Zaltash, and S. Dhodapkar. 1989. A simplified correlation for solids friction factor in horizontal conveying systems based on Yang's unified theory. Powder Technology 58: 187–193.

Levy, A. and Mason, D.J., 2000. Two-layer model for non-suspension gas–solids flow in pipes. Powder technology, 112(3), pp.256-262.

Mallick, S. S., and P. W. Wypych. 2009. Modeling solid friction for dense phase pneumatic conveying of powders. Particulate Science and Technology 27: 444–455.

Mason, D.J., 1991. A study of the modes of gas-solids flow in pipelines (Doctoral dissertation, Thames Polytechnic).

Molerus, O. 1996. Overview: Pneumatic transport of solids. Powder Technology 88: 309–321.

Molerus, O., 1982. Interpretation of Geldart's type A, B, C and D powders by taking into account interparticle cohesion forces. Powder technology, 33(1), pp.81-87.

Narsimhan, G., 1965. On a generalized expression for prediction of minimum fluidization velocity. AIChE Journal, 11(3), pp.550-554.

Patwardhan, V.S. and Tien, C., 1985. Sedimentation and liquid fluidization of solid particles of different sizes and densities. Chemical Engineering Science, 40(7), pp.1051-1060.

Rautiainen, A., and P. Sarkomaa. 1998. Solid friction factors in a upward lean gas-solids flows. Powder Technology 95: 25–35.

Setia, G., Mallick, S.S., Pan, R. and Wypych, P.W., 2016. Modeling solids friction factor for fluidized dense-phase pneumatic transport of powders using two layer flow theory. Powder Technology, 294, pp.80-92.

Seville, J., Tüzün, U. and Clift, R., 2012. Processing of particulate solids (Vol. 9). Springer Science & Business Media.

Shampine, L.F. and Reichelt, M.W., 1997. The matlab ode suite. SIAM journal on scientific computing, 18(1), pp.1-22.

Srivastava, A. and Sundaresan, S., 2003. Analysis of a frictional–kinetic model for gas–particle flow. Powder technology, 129(1), pp.72-85.

Stegmaier, W. 1978. Zur Berechnung der Horizontalen Pneumatischen Forderung Feinko ¨rniger Stoffe. Fo ¨rdern und Heben 28: 363–366.

Van Heerden, C., Nobel, A.P.P. and Van Krevelen, D.W., 1951. Studies on fluidization. I—the critical mass velocity. Chemical Engineering Science, 1(1), pp.37-49.

Wang, Z., Kwauk, M. and Li, H., 1998. Fluidization of fine particles. Chemical Engineering Science, 53(3), pp.377-395.

Weber, M. 1981. Principles of hydraulic and pneumatic conveying in pipes. Bulk Solids Handling 1: 57–63.

Williams, K. C. 2008. Dense phase pneumatic conveying of powders: Design aspects and phenomena. PhD thesis, University of Newcastle, Australia.

Wilson, K.C., 1976, May. A unified physically-based analysis of solid-liquid pipeline flow. In Proceedings Hydrotransport (Vol. 4, pp. 1-16).

Wypych, P., and P. C. Arnold. 1987. On improving scale-up procedures for pneumatic conveying design. Powder Technology 50: 181–294. Yang, W. C. 1974. Correlations of solid friction factors in vertical and horizontal pneumatic conveying. AIChE Journal 20: 605–607.

Xu, C.C. and Zhu, J., 2008. Prediction of the minimum fluidization velocity for fine particles of various degrees of cohesiveness. Chemical Engineering Communications, 196(4), pp.499-517.

Yates, J.G., 1996. Effects of temperature and pressure on gas-solid fluidization. Chemical Engineering Science, 51(2), pp.167-205.

Geldart, D. (1973). "Types of gas fluidization". Powder technology. 7 (5): 285–292

Appendix: MATLAB Scripts

EQUATION-1

```
input= xlsread ('eqn1')
x= input (:,1);
S= input(:,2);
Rho_g1=input (:,3);
A_1=input (:,4);
h=input (:,5);
Rho_s=input (:,6);
DP_1=input (:,7);
fori= 1:6
   T1(i)= ((Rho_g1(i)*A_1(i))*exp(((S(i)*h(i)*x(i))/(2*A_1(i)))+1.234));
% c1(i) = exp(((S(i)*h(i)*x(i))/(2*A_1(i)))+1.234);
% c2(i) = Rho_g1(i) *A_1(i);
% T1(i)=c1(i)*c2(i);

%T1(i)= Rho_g1(i)*A_1(i)*(exp(S((i)*h(i)*x(i)))/(2*A_1(i))+1.234);
   T2(i)=(0.5*Rho_g1(i)*S(i)*h(i)*exp(((S(i)*h(i)*x(i))/(2*A_1(i)))+1.234));
   T3(i)=A_1(i)*DP_1(i)*exp(((S(i)*h(i)*x(i))/(2*A_1(i)))+1.234);
   T4(i)=25000*A_1(i)*Rho_g1(i)*exp((1/(2*A_1(i)*Rho_s(i))*S(i)*h(i)*x(i))+1)*
((24/(0.09*Rho_g1(i)))*(1+0.15*((0.09*Rho_g1(i))^(0.1687))))+(0.42/(1+42500*
((0.09*Rho_g1(i))^(-1.16))));
end
```

EQUATION- 2

```
input= xlsread ('eqn2')
x= input (:,1);
Rho_g1= input (:,2);
Rho_g2=input (:,3);
A_2=input (:,4);
S=input (:,5);
Rho_s=input (:,6);
DP_1=input (:,7);
```

```
f_gi=input (:,8);
f_si=input (:,9);
f_s1=input (:,10);
h=input (:,11);
A_1=input (:,12);
S_1=input (:,13);
fori= 1:6
   T1(i)=(Rho_s(i)*A_1(i)* exp(((S(i)*h(i)*x(i))/(2*A_1(i)*Rho_s(i)))+1));
   T2(i)=0.5*Rho_s(i)*S(i)*h(i)*(exp(((S(i)*h(i)*x(i))/(2*A_1(i)*Rho_s(i)))+1));
   T3(i)=1150 * S_1(i) * f_s1(i) * exp (((S(i)*h(i)*x(i))/(2*A_1(i)*Rho_s(i)))+1);
 c1(i)= ((((-1)*Rho_g1(i)*S(i)*h(i)*x(i))/(2*A_2(i)*Rho_g2(i)))*
exp(((S(i)*h(i)*x(i))/(2*A_1(i)))+1.23)+11.23);
c2(i)=f_gi(i)*0.5*Rho_g2(i);
 c3(i)=exp(((S(i)*h(i)*x(i))/(2*Rho_g1(i)*A_1(i)))+1.23);
c4(i)=S(i);
t4(i)=c1(i)*c2(i)*c3(i)*c4(i);
T4(i)=t4(i);
 d1(i)=((((-0.5)*S(i)*h(i)*x(i))/(A_2(i))))*exp(((S(i)*h(i)*x(i))/(2*A_1(i)))+1);
d2(i)=f_si(i)*0.5*Rho_s(i);
 d3(i)=exp(((S(i)*h(i)*x(i))/(2*A_1(i)))+1);
d4(i)=S(i);
  t5=d1.*d2.*d3.*d4;
T5 =t5;
T6(i)=A_1(i)*DP_1(i)*exp(((S(i)*h(i)*x(i))/(2*A_1(i)*Rho_s(i)))+1);
T7(i)=25000*A_1(i)*Rho_g1(i)*exp((1/(2*A_1(i)*Rho_s(i))*S(i)*h(i)*x(i))+1)*((24/(0.09*
Rho_g1(i)))*(1+0.15*((0.09*Rho_g1(i))^(0.1687))))+(0.42/(1+42500*((0.09*Rho_g1(i))^(-
1.16))));
End
```

EQUATION- 3

```
input= xlsread ('eqn3')
x= input (:,1);
S= input (:,2);
Rho_g1=input (:,3);
Rho_g2=input (:,4);
```

```
A_1=input (:,5);
A_2=input (:,6);
h=input (:,7);
Rho_s=input (:,8);
D_P2=input (:,9);
f_gi=input (:,10);
f_g2=input (:,10);
S_2=input (:,11);
fori= 1:6
T1(i)=((((-1)*Rho_g1(i)*S(i)*h(i)*x(i))/(2*A_2(i)*Rho_g2(i)))*
exp(((S(i)*h(i)*x(i))/(2*A_1(i)))+1.23)+11.23)*Rho_g2(i)*A_2(i));
T2(i)= ((-1)*0.5*Rho_g1(i)*S(i)*h(i)*exp(((S(i)*h(i)*x(i))/(2*A_1(i)))+1.23));
T3(i)=((((-1)*Rho_g1(i)*S(i)*h(i)*x(i))/(2*A_2(i)*Rho_g2(i)))*
exp(((S(i)*h(i)*x(i))/(2*A_1(i)))+1.23)+11.23)*(f_g2(i)*0.5*Rho_g2(i))*S_2(i);
c1(i)= ((((-1)*Rho_g1(i)*S(i)*h(i)*x(i))/(2*A_2(i)*Rho_g2(i)))*
exp(((S(i)*h(i)*x(i))/(2*A_1(i)))+1.23)+11.23);
c2(i)=f_gi(i)*0.5*Rho_g2(i);
c3(i)=exp(((S(i)*h(i)*x(i))/(2*Rho_g1(i)*A_1(i)))+1.23);
c4(i)=S(i);
t4=c1(i).*c2(i).*c3(i).* c4(i);
T4=t4;
T5(i)=(((((-1)*Rho_g1(i)*S(i)*h(i)*x(i))/(2*A_2(i)*Rho_g2(i)))*
exp(((S(i)*h(i)*x(i))/(2*A_1(i)))+1.23)+11.23))*A_2(i)*D_P2(i);
T6(i)= 25000*A_2(i)*Rho_g2(i)*((((-
1)*Rho_s(i)*S(i)*h(i))/(2*A_2(i)*Rho_g2(i)))*exp(((S(i)*h(i)*x(i))/(2*A_1(i)))+1))*((24/(0.
09*Rho_g2(i)))*(1+0.15*((0.09*Rho_g2(i))^(0.1687))))+(0.42/(1+42500*((0.09*Rho_g2(i))
^(-1.16))));
End
```

EQUATION- 4

```
input= xlsread ('eqn4')
x = input (:,1);
h =input (:,2);
S =input (:,3);
```

```
A_1 =input (:,4);
A_2 =input (:,5);
Rho_s =input (:,6);
Rho_g2=input (:,7);
D_P2 =input (:,8);
f_si=input (:,9);

for i= 1:6;
   T1(i)= ((((-
0.5)*S(i)*h(i)*x(i))/(A_2(i))))*exp(((S(i)*h(i)*x(i))/(2*A_1(i)))+1)*Rho_s(i)*A_2(i);
   T2(i)= 0.5*Rho_s(i)*S(i)*h(i)*(exp(((S(i)*h(i)*x(i))/(2*A_1(i)*Rho_s(i)))+1));
    d1(i)=((((-0.5)*S(i)*h(i)*x(i))/(A_2(i))))*exp(((S(i)*h(i)*x(i))/(2*A_1(i)))+1);
d2(i)=f_si(i)*0.5*Rho_s(i);
 d3(i)=exp(((S(i)*h(i)*x(i))/(2*A_1(i)))+1);
d4(i)=S(i);
  t3=d1.*d2.*d3.*d4;
  T3 =t3;
   T4(i)=A_2(i)*D_P2(i)*((((-
0.5)*S(i)*h(i)*x(i))/(A_2(i))))*exp(((S(i)*h(i)*x(i))/(2*A_1(i)))+1);
   T5(i)= 25000*A_2(i)*Rho_g2(i)*((((-
1)*Rho_s(i)*S(i)*h(i))/(2*A_2(i)*Rho_g2(i)))*exp(((S(i)*h(i)*x(i))/(2*A_1(i)))+1))*((24/(0.
09*Rho_g2(i)))*(1+0.15*((0.09*Rho_g2(i))^(0.1687))))+(0.42/(1+42500*((0.09*Rho_g2(i))
^(-1.16))));
end
```

MATLAB Program

```
rho_s=300;
%[t,y] = ode45(@(z,y) f(z,y),[0 1],[u_s;u_a;ep_s]);
_
_
_
u_s=y(:,1)
u_a=y(:,2)
ep_s=y(:,3)
y(:,5)=1-y(:,3);    % ep_a
_
_
%Ploting of the graph
% plot(x,y(:,1),'k-',x,y(:,2),'k--',x,y(:,3),'r-','linewidth',2);
% legend('u_{s}','u_{a}, '\epsilon_{s}')
_
_
% defining the set of Ist order differential equation.
function dydx =f(x,y)
global f_a f_s rho_a rho_s dPdx drho_adx
----
------
dydx=[y(1).*bracket_term./(y(3).*denominator);
     -y(2).*bracket_term./((1-y(3)).*denominator)-y(2).*drho_adx/rho_a;
     -1*bracket_term./denominator];
```